Relay Assisted Cooperative Ambient Backscatter Communication with Hybrid Long-Short Packets

Xi Song, Dongsheng Han, Liqin Shi, Haijian Sun, Member, IEEE, and Rose Qingyang Hu, Fellow, IEEE

Abstract-In this paper, we investigate a relay-assisted cooperative ambient backscatter communication network, where the primary transmitter (PT) and the backscatter transmitter (BT) transmit a long packet with an infinite blocklength and a short packet with a finite blocklength to an information receiver (IR) with the aid of a relay node, respectively. Considering the energy causality constraint and the decoding error in the process of successive interference cancellation (SIC), we derive the expressions for PT's outage probability and BT's average block error rate (BLER). The analytical results show that the fixed SIC decoding scheme considered at IR may lead to a poor performance for both the outage probability and the average BLER. To address it, we propose an improved SIC decoding scheme and evaluate its achievable transmission performance by deriving the expressions for PT's outage probability and BT's average BLER. Computer simulations verify our derivations, confirm the superior performance of the improved SIC decoding scheme compared to the fixed one, and provide insights into the influences of different parameters (e.g., PT's transmission power, BT's power reflection coefficient, power allocation of the relay node) on the achievable outage probability and average BLER. Particularly, increasing the short-packet blocklength enhances the BLER performance of BT. However, it does not necessarily improve the outage performance of PT.

Index Terms—Ambient backscatter communication, long packet with an infinite blocklength, short packet with a finite blocklength, outage probability, average block error rate.

I. Introduction

To achieve pervasive connectivity, massive low-power Internet of Things (IoT) nodes, which are tasked with the functions of data sensing, generation, and transmission, will be deployed worldwide to facilitate the delivery of diverse intelligent services and applications [1]–[3]. Among all technical challenges for enabling massive low-power IoT nodes deployment, two predominant aspects have emerged. One is the limited available spectrum resource, and the other is the short operational life of the battery-powered IoT nodes. To address the above two challenges, ambient backscatter communication (AmBackCom) has been proposed. In AmBackCom, the IoT node, functioning as a backscatter transmitter (BT), can not

Xi Song and Dongsheng Han are with the school of Electrical and Electronic Engineering, North China Electric Power University. (email: 120212501020@ncepu.edu.cn; handongsheng@ncepu.edu.cn)

Liqin Shi is with the Shaanxi Key Laboratory of Information Communication Network and Security, Xi'an University of Posts & Telecommunications, Shannxi, China. (email: liqinshi@hotmail.com)

Haijian Sun is with the School of Electrical and Computer Engineering, The University of Georgia, Athens, GA, USA. (email: hsun@uga.edu)

Rose Qingyang Hu is with the Department of Electrical and Computer Engineering at Utah State University, UT, USA. (email: rose.hu@usu.edu)

This work was supported by the National Natural Science Foundation of China under Grant 62301421.

only modulate its information on primary signals (e.g., cellular signals), rather than generating carrier signals by itself, to achieve information transmission, but also harvest energy from primary signals to prolong its operational life [4], [5].

Many studies have investigated the performance of Am-BackCom such as the outage probability and the ergodic capacity. In [6], the authors considered a RF-powered cognitive radio network with AmBackCom, and analyzed the coverage probabilities and ergodic capacity for both primary and AmBackCom users. The authors in [7] investigated the outage performance of a wireless powered cognitive relay network with AmBackCom. The authors in [8] studied the outage performance for wireless powered device-to-device (D2D) communication with AmBackCom, where a hybrid D2D transmitter alternately operates in the backscatter mode and the harvest-then-transmit (HTT) mode. Considering the co-channel interference between the primary transmission and AmBackCom, the authors in [9] derived the closed-form expressions of the outage probability for both the primary transmission and AmBackCom in a single-cell cellular network. Using stochastic geometry, the authors in [10] extended the work [9] to a multi-cell cellular network and studied the successful transmission probabilities for the primary transmission and AmBackCom.

In the above works [6]–[10], it has been demonstrated that the performance of AmBackCom is largely limited by the co-channel interference, which encourages us to consider the cooperation between the primary and AmBackCom links for suppressing the co-channel interference. To date, the performance of various cooperative AmBackCom has been studied. For example, the authors in [11] considered a cooperative AmBackCom that operates in the commensal, parasitic, or competitive mode, and derived closed-form expressions of the outage probability for both primary and AmBackCom links. The authors in [12] proposed an opportunistic source selection based two-way cooperative AmBackCom system and investigated the outage probabilities for both primary and AmBackCom links. In [13], the authors investigated the upper bounds of the ergodic rate for the primary transmission and AmBackCom in a cooperative AmBackCom system. The authors in [14] studied the scaling behavior of the outage probability and ergodic capacity in a cooperative AmBackCom. Taking the impact of the energy outage at BT into consideration, the authors in [15] derived the ergodic sum capacity of both primary and backscatter transmissions. Integrating intelligent reflecting surface with AmBackCom, the authors in [16] derived the analytical expressions for the coverage probability and the average throughput. The average bit error rate was derived in a similar system in [17]. Combining nonorthogonal multiple access (NOMA) with AmBackCom, the authors in [18] derived the outage probabilities of the two NOMA signals and the AmBackCom signal.

We note that existing works [6]–[18] assumed a long data packet with an infinite blocklength for both AmBackCom and primary transmissions. However, in most IoT applications (e.g., factory automation, intelligent transportation and smart grids), BT usually transmits a short data packet with a finite blocklength [19]. As Shannon capacity is not applicable for finite blocklength [20]-[23], cooperative AmBackCom with hybrid long and short packets¹, in which a long data packet is transmitted by the primary transmitter (PT) while BT modulates its short-packet data on the received primary signals and then backscatters them, should be re-studied. In [24], the authors proposed two resource allocation schemes to minimize the transmit power of PT and maximize the system energy efficiency for a cooperative AmBackCom network with hybrid long and short packets, respectively. The authors in [25] analyzed the average block error rate (BLER) for a cooperative AmBackCom network with hybrid long and short packets and proposed a resource allocation scheme to improve transmission reliability. However, there are still some research gaps need to be filled.

- The work [25] assumed that the primary signal is always decoded correctly when deriving the BLER, i.e., the decoding error in the process of successive interference cancellation (SIC)², has not been considered. In practice, SIC decoding error is common due to many factors such as low SNR. Therefore, if the receiver adopts SIC to decode both primary and AmBackCom signals sequentially, such decoding error will have a significant impact on the AmBackCom's BLER, which is not negligible.
- In cooperative AmBackCom, it is expected that BT is self-powered. This motivates us to consider the energy causality constraint at BT in assessing the transmission performance, while this has not been considered in [25].
- Existing studies [24], [25] assumed that there exist direct links for both the primary transmission and AmBackCom links, while the direct links may not exist due to severe path loss, shadowing and receiver sensitivity. In this case, it is necessary to consider relay in the cooperative AmBackCom with hybrid long and short packets.

In this work, we plan to directly address above gaps and study the performance for a relay-assisted cooperative Am-BackCom network³, where the long data packets transmitted by PT and the short data packets backscattered by BT are forwarded to the information receiver (IR) with the help of a decode-and-forward (DF) relay (R). Our main contributions are summarized as follows.

¹We note that the short packet has been considered in few works (e.g., [22], [23]), but they have not considered the hybrid long and short packet and thus have not been reviewed here.

²Note that the SIC decoding error comes from the unsuccessful decoding of the signal who is decoded first.

³Although there are some works considering relay and AmBackCom as a whole (see [26]–[29]), they have not considered the cooperative AmBackCom with practical hybrid long and short packets and thus differ from our considered network.

- We analyze the outage performance for the primary transmission and the BLER of AmBackCom while considering both the energy causality constraint at BT and the decoding error of SIC. Specifically, we derive the closedform expressions for the outage probability of the primary transmission and the average BLER of AmBackCom. The derived expressions provide practical design insights into the effects of different parameters on the outage probability and the average BLER.
- The above expressions are derived based on a fixed SIC decoding scheme at IR, where IR first decodes PT's information and then decodes BT's information after cancelling the decoded PT's information. In this case, a poor outage performance or BLER occurs when IR fails to decode PT's information. To address it, we consider an improved SIC decoding scheme at IR. Under this setting, we re-derive the closed-form expressions for the outage probability of the primary transmission and the average BLER of AmBackCom.
- Simulation results show the following five facts. Firstly, as the short-packet blocklength increases, the average BLER for AmBackCom initially decreases and then converges to a specific value. Meanwhile, the outage probability of the primary transmission may increase or decrease, depending on the power allocated for forwarding primary signals at R. Secondly, when the power allocated for forwarding primary signals at R is below a certain threshold, the outage probability of the primary transmission tends to increase along with PT's transmit power. Thirdly, compared with the fixed SIC decoding scheme, the improved SIC decoding scheme can significantly improve both the outage performance of the primary transmission and the error performance of AmBackCom. Fourthly, there exists an optimal power reflection coefficient at BT that minimizes the average BLER of AmBackCom. It should be noted that this optimal power reflection coefficient cannot be located at the boundary. Lastly, there exist the optimal locations of R for minimizing the outage probability of the primary transmission and the average BLER of AmBackCom, respectively. Specifically, the optimal location for minimizing the average BLER is closer to BT compared with the optimal location that minimizes the outage probability.

The remainder of this paper is organized as follows. The system model is provided in Section II. Sections III and IV analyze the outage performance of the primary transmission and the error performance of AmBackCom, respectively. In Section V, an improved SIC decoding scheme at IR is proposed and the corresponding outage probability and BLER are derived. Simulation results are shown in Section VI, followed by conclusions in Section VII.

II. SYSTEM MODEL

As shown in Fig. 1, this work considers a relay assisted cooperative AmBackCom network. The whole network is composed of one PT, one BT, one DF relay R, and one

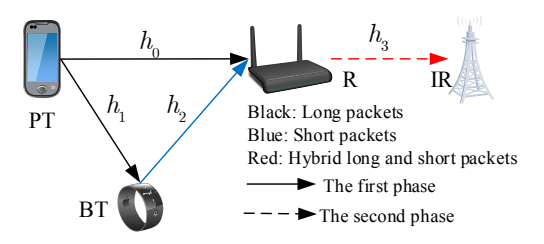


Fig. 1. System model.

IR, where R is used to assist PT's and BT's information transmissions since there is no direct links between PT/BT and IR due to severe path loss. We consider that with the help of R, PT transmits long data packets to IR while BT backscatters short data packets to IR via AmBackCom. Let h_0 , h_1 , h_2 , and h_3 represent the small-scale channel gains of the PT-R link, the PT-BT link, the BT-R link, and the R-IR link, respectively. Then the channel gains of the PT-R link, the PT-BT link, the BT-R link, and the R-IR link are respectively given by $h_0 d_0^{-\alpha_0}$, $h_1d_1^{-\alpha_1}$, $h_2d_2^{-\alpha_2}$, and $h_3d_3^{-\alpha_3}$, where d_0 , d_1 , d_2 , and d_3 are the distances from PT to R and BT, and from R to BT and IR, and α_0 , α_1 , α_2 , and α_3 are the corresponding path loss exponents. Here we assume that all channels are quasi-static and subject to Rayleigh fading, and the corresponding channel gains follow the exponential distribution, i.e., $h_k \sim \exp(\frac{1}{\lambda_k})$ with the scale parameter of the exponential distribution λ_k , $k \in \{0, 1, 2, 3\}$ [9]. Note that the channel estimation for h_0 , h_1 , h_2 and h_3 can be realized as follows. Firstly, both h_0 and h_3 can be obtained by using several existing channel estimation methods, e.g., least-square estimation. Then the channel estimation method in [30] can be used to obtain h_1 and h_2 .

A full transmission block T is divided into two equal phases. In the first phase with the duration of $\frac{T}{2}$, PT transmits N_s symbols carrying the information, denoted as s, with unit power to R. Here we assume N_s is sufficiently large such that the transmitted packet by PT can be regarded as a long one. Meanwhile, BT receives the signal transmitted by PT and divides the received signal into two parts through a power reflection coefficient $\beta,\beta\in[0,1]$: one part for backscattering and the remaining part for energy harvesting (EH). Thus, the harvested energy at BT is given by

$$E_{\rm BT} = F_{\rm NL}(P_r) \frac{T}{2},\tag{1}$$

where $P_r=(1-\beta)P_0h_1d_1^{-\alpha_1}$ is the received signal power for EH at BT with PT's transmit power P_0 , and $F_{\rm NL}(P_r)$ denotes the function of the energy harvester's output power at BT with respect to the input power P_r . Here the specific function $F_{\rm NL}(P_r)$ is not explicitly provided in order to achieve a broader comprehension of overall performance.

Let $P_{\rm c}$ denote the constant circuit power consumption at BT. Assume that BT only uses its harvested energy to perform AmBackCom, then there exist the following two cases.

(a) If $E_{\rm BT} \geq \frac{P_c T}{2}$ is satisfied, BT is active and backscatters its information symbol c with blocklength N_c and $\mathbb{E}[|c|^2]=1$. In this case, R receives the signals from both PT and BT, and

thereby the received signal can be expressed as

$$y_{\rm R}^{\rm a} = \sqrt{P_0 h_0 d_0^{-\alpha_0}} s + \sqrt{\beta P_0 h_1 h_2 d_1^{-\alpha_1} d_2^{-\alpha_2}} sc + n_{\rm R},$$
 (2)

where $n_{\rm R} \sim \mathcal{CN}(0,\sigma^2)$ is the additive white Gaussian noise (AWGN) at R.

In this case, R decodes s and c by performing SIC. Here we assume R first decodes s by treating $\sqrt{\beta P_0 h_1 h_2 d_1^{-\alpha_1} d_2^{-\alpha_2}} sc$ as an interference signal, then removes $\sqrt{P_0 h_0 d_0^{-\alpha_0}} s$ via SIC, and finally decodes c from the remaining signal $\sqrt{\beta P_0 h_1 h_2 d_1^{-\alpha_1} d_2^{-\alpha_2}} sc + n_{\rm R}$. Thus, the signal-to-interference-plus-noise ratio (SINR) for decoding s equals

$$\gamma_{\mathbf{R},s}^{\mathbf{a}} = \frac{P_0 h_0 d_0^{-\alpha_0}}{\beta P_0 h_1 h_2 d_1^{-\alpha_1} d_2^{-\alpha_2} + \sigma^2}.$$
 (3)

If s is decoded and $\sqrt{P_0h_0d_0^{-\alpha_0}s}$ is successfully removed via SIC from $y_{\rm R}^{\rm a}$, the signal-to-noise ratio (SNR) for decoding c can be written as

$$\gamma_{R,c}^{a} = \frac{\beta P_0 h_1 h_2 d_1^{-\alpha_1} d_2^{-\alpha_2}}{\sigma^2}.$$
 (4)

(b) If $E_{\rm BT} < P_{\rm c} \rho T$ holds, BT remains silent. In this case, R only receives PT's signal, i.e.,

$$y_{\rm R}^{\rm b} = \sqrt{P_0 h_0 d_0^{-\alpha_0}} s + n_{\rm R}.$$
 (5)

Using (5), the SNR for decoding s is given by

$$\gamma_{R,s}^{b} = \frac{P_0 h_0 d_0^{-\alpha_0}}{\sigma^2}.$$
 (6)

In the second phase with the duration of $\frac{T}{2}$, R will transmit its decoded information with its transmit power P_R . Based on the decoded signals at R, there exist three cases for the R's information transmission.

Case I: If both s and c are decoded successfully, then R transmits the decoded information symbols, denoted by \widehat{s} and \widehat{c} , to IR. In this case, the received signal at IR is expressed as

$$y_{\rm IR}^{\rm I} = \left(\sqrt{a_s}\hat{s} + \sqrt{1 - a_s}\hat{c}\right)\sqrt{P_{\rm R}h_3d_3^{-\alpha_3}} + n_{\rm IR},\tag{7}$$

where $0 \le a_s \le 1$ denotes the power allocation ratio for \widehat{s} , and $n_{\rm IR} \sim \mathcal{CN}(0,\sigma^2)$ is the AWGN at IR. Here, a low-complexity fixed SIC decoding scheme⁵ is considered at IR, where IR decodes \widehat{s} first and then decodes \widehat{c} after cancelling $\sqrt{a_s P_{\rm R} h_3 d_3^{-\alpha_3}} \widehat{s}$. Accordingly, the SINR for decoding \widehat{s} is given by

$$\gamma_{\text{IR},s}^{\text{I}} = \frac{a_s P_{\text{R}} h_3 d_3^{-\alpha_3}}{(1 - a_s) P_{\text{R}} h_3 d_3^{-\alpha_3} + \sigma^2}.$$
 (8)

⁴The reasons for this assumption are two-fold. First, the received signal backscattered by BT is usually weaker than that transmitted by PT due to the double path loss existing in AmBackCom [9], [10]. Second, the BLER is always larger than zero for short packet communications when the transmission rate is smaller than the Shannon rate but can be equal to zero for long packet communications [21].

 5 In this scheme, the initially decoded information is consistently treated as \widehat{s} , removing the necessity to ascertain whose information it is based on the value of a_{s} fed back by R and the requirement for the feedback information at IR. Thus, the fixed SIC decoding scheme enjoys a low operational complexity.

Similarly, the SNR for decoding \hat{c} , after removing \hat{s} from $y_{\rm IR}^{\rm I}$ via SIC, is written as

$$\gamma_{\text{IR},c}^{\text{I}} = \frac{(1 - a_s) P_{\text{R}} h_3 d_3^{-\alpha_3}}{\sigma^2}.$$
(9)

Case II: If R receives both c and s but fails to decode c, or R only receives and decodes s successfully, then only \widehat{s} can be transmitted by R. In this case, the received signal at IR is expressed as

$$y_{\rm IR}^{\rm II} = \sqrt{P_{\rm R} h_3 d_3^{-\alpha_3}} \hat{s} + n_{\rm IR}.$$
 (10)

Accordingly, the SNR for decoding \hat{s} is given by

$$\gamma_{\mathrm{IR},s}^{\mathrm{II}} = \frac{P_{\mathrm{R}} h_3 d_3^{-\alpha_3}}{\sigma^2}.\tag{11}$$

Case III: If R fails to decode s, then no signals can be received at IR. In this case, both PT and BT fail to transmit their information to IR.

III. OUTAGE ANALYSIS FOR PRIMARY TRANSMISSION

This section will analyze the outage performance of the primary transmission. Assume that PT transmits long data packets of $R_{\rm th}$ bits per channel use, then the given threshold for decoding both s and \widehat{s} at R and IR is given by $\gamma_{\rm th}=2^{R_{\rm th}}-1$. Denote $\Omega_{i,{\rm fail}}, i\in\{{\rm R,IR}\}$ as the event that i fails to decode the short-packet information and $\varepsilon_{i,c}$ as the probability that $\Omega_{i,{\rm fail}}$ happens under given $\gamma_{i,c}^j, \{i,j\} \in \{\{{\rm R,a}\}, \{{\rm IR,I}\}\}$. Based on [20], $\varepsilon_{i,c}$ under a sufficiently large blocklength, e.g., $N_c \geq 100$, can be closely approximated as

$$\varepsilon_{i,c} \approx Q \left(\sqrt{\frac{N_c}{V\left(\gamma_{i,c}^j\right)}} \left(C\left(\gamma_{i,c}^j\right) - \frac{B_c}{N_c} \right) \right) \stackrel{\Delta}{=} \Psi\left(\gamma_{i,c}^j\right),$$
(12)

where $Q\left(\cdot\right)$ is the Gaussian Q function, $V\left(\gamma_{i,c}^{j}\right)=\left(1-\frac{1}{\left(1+\gamma_{i,c}^{j}\right)^{2}}\right)\left(\log_{2}e\right)^{2}$ is the channel dispersion, $C\left(\gamma_{i,c}^{j}\right)=\log_{2}\left(1+\gamma_{i,c}^{j}\right)$ is the Shannon capacity, and $\frac{B_{c}}{N_{c}}$ denotes the BT's rate with the number of bits B_{c} and the short-packet blocklength N_{c} . It can be observed that $\varepsilon\leq0.5$ holds when the capacity is larger than the rate, i.e., $C\left(\gamma\right)\geq\frac{B_{c}}{N_{c}}$, and that $\varepsilon>0.5$ holds when the capacity is lower than the rate, i.e., $C\left(\gamma\right)<\frac{B_{c}}{N_{c}}$.

Let $P_{\mathrm{out,p}}$ denote the outage probability of the primary transmission and it can be computed as $P_{\mathrm{out,p}} = 1 - P_{\mathrm{suc,p}}$, where $P_{\mathrm{suc,p}}$ is PT's successful transmission probability. In order to realize PT's successful transmission, \widehat{s} in Case I or II should be successfully decoded. Considering the energy causality constraint at the BT and the fixed SIC decoding

scheme, $P_{\text{suc,p}}$ can be calculated as

$$P_{\text{suc,p}} = \underbrace{\mathbb{P}\left(E_{\text{BT}} \ge \frac{P_{\text{c}}T}{2}, \gamma_{\text{R},s}^{\text{a}} \ge \gamma_{\text{th}}, \Omega_{\text{R,suc}}, \gamma_{\text{IR},s}^{\text{I}} \ge \gamma_{\text{th}}\right)}_{P_{1}} + \underbrace{\mathbb{P}\left(E_{\text{BT}} \ge \frac{P_{\text{c}}T}{2}, \gamma_{\text{R},s}^{\text{a}} \ge \gamma_{\text{th}}, \Omega_{\text{R,fail}}, \gamma_{\text{IR},s}^{\text{II}} \ge \gamma_{\text{th}}\right)}_{P_{2}} + \underbrace{\mathbb{P}\left(E_{\text{BT}} < \frac{P_{\text{c}}T}{2}, \gamma_{\text{R},s}^{\text{b}} \ge \gamma_{\text{th}}, \gamma_{\text{IR},s}^{\text{II}} \ge \gamma_{\text{th}}\right)}_{P_{3}}, \quad (13)$$

where $\Omega_{\mathrm{R,suc}}$ refers to the event that R can decode c successfully and happens under given $\gamma_{\mathrm{R,}c}^{\mathrm{a}}$ with the probability $1-\varepsilon_{\mathrm{R,}c}$, P_1 is PT's successful transmission probability in Case I, P_2 is the successful transmission probability in Case II with $E_{\mathrm{BT}} \geq \frac{P_{\mathrm{c}}T}{2}$, and P_3 is the successful transmission probability in Case II with Case II with $E_{\mathrm{BT}} < \frac{P_{\mathrm{c}}T}{2}$. It can be observed from (13) that both E_{BT} and $\gamma_{\mathrm{R,su}}^{\mathrm{a}}$ involves h_1 , and the probabilities that both $\Omega_{\mathrm{R,suc}}$ and $\Omega_{\mathrm{R,fail}}$ happen are highly related with h_1 . Thus, it is very challenging to derive $P_{\mathrm{out,p}}$.

A. Derivation of P_1

Based on (13), P_1 can be rewritten as (14), as shown at the top of this page, where $A_1 = \frac{d_1^{\alpha_1} F_{\rm NL}^{-1}(P_c)}{(1-\beta)P_0}$, $A_2 = \gamma_{\rm th}\beta d_1^{-\alpha_1}d_2^{-\alpha_2}d_0^{\alpha_0}$, $A_3 = \frac{\gamma_{\rm th}\sigma^2 d_0^{\alpha_0}}{P_0}$, and $A_4 = \frac{\gamma_{\rm th}\sigma^2 d_3^{\alpha_3}}{P_{\rm R}}$. It is obvious that when $a_s - \gamma_{\rm th}(1-a_s) \leq 0$, i.e., $0 \leq \alpha_s < \gamma_{\rm th}$ holds. The second s

It is obvious that when $a_s - \gamma_{\rm th} (1-a_s) \leq 0$, i.e., $0 \leq a_s \leq \frac{\gamma_{\rm th}}{1+\gamma_{\rm th}}$ holds, $\mathbb{P}\left((a_s - \gamma_{\rm th} (1-a_s)) \, h_3 \geq A_4\right)$ equals 0, leading to $P_1 = 0$. Otherwise, when $\frac{\gamma_{\rm th}}{1+\gamma_{\rm th}} < a_s \leq 1$, P_1 then becomes

$$P_{1} = \mathbb{P}\left(h_{1} \geq A_{1}, h_{0} \geq A_{2}h_{1}h_{2} + A_{3}, \Omega_{R,suc}\right)$$

$$\times \mathbb{P}\left(h_{3} \geq \frac{A_{4}}{a_{s} - \gamma_{th}\left(1 - a_{s}\right)}\right)$$

$$= \exp\left(-\frac{A_{4}}{\left(a_{s} - \gamma_{th}\left(1 - a_{s}\right)\right)\lambda_{3}}\right) \left(P_{11} - P_{12}\right), \quad (15)$$

where $P_{11} = \mathbb{P}(h_1 \ge A_1, h_0 \ge A_2 h_1 h_2 + A_3)$ and $P_{12} = \mathbb{P}(h_1 \ge A_1, h_0 \ge A_2 h_1 h_2 + A_3, \Omega_{\text{R,fail}})$.

In the following, we first provide the probability density function (PDF) of h_1h_2 in **Lemma 1**, and then derive the expressions of P_{11} and P_{12} , respectively.

Lemma 1 [9]: Since $h_k \sim \exp(\frac{1}{\lambda_k}), k \in \{1, 2\}$, the PDF of h_1h_2 , denoted by $f_{h_1h_2}(y)$, is given by

$$f_{h_1 h_2}(y) = \frac{2}{\lambda_1 \lambda_2} K_0 \left(2\sqrt{\frac{y}{\lambda_1 \lambda_2}} \right), \tag{16}$$

where $K_0(\cdot)$ is the modified Bessel function of the second kind [31].

Based on **Lemma 1**, we can derive P_{11} as

$$P_{11} = \mathbb{P}(h_{1} \geq A_{1}, h_{0} \geq A_{2}h_{1}h_{2} + A_{3})$$

$$= \int_{A_{1}}^{+\infty} f_{h_{1}}(x) \int_{0}^{+\infty} f_{h_{1}h_{2}}(y) \int_{A_{2}y+A_{3}}^{+\infty} f_{h_{0}}(z) dz dy dx$$

$$= \exp\left(-\frac{A_{1}}{\lambda_{1}}\right) \int_{0}^{+\infty} f_{h_{1}h_{2}}(y) \exp\left(-\frac{A_{2}y+A_{3}}{\lambda_{0}}\right) dy$$

$$\stackrel{\text{(aa)}}{=} -\theta \exp\left(\theta - \frac{A_{1}}{\lambda_{1}} - \frac{A_{3}}{\lambda_{0}}\right) \text{Ei}(-\theta), \tag{17}$$

$$P_{1} = \mathbb{P}\left(h_{1} \geq A_{1}, h_{0} \geq A_{2}h_{1}h_{2} + A_{3}, \Omega_{R,suc}, (a_{s} - \gamma_{th}(1 - a_{s})) h_{3} \geq A_{4}\right)$$

$$= \mathbb{P}\left(h_{1} \geq A_{1}, h_{0} \geq A_{2}h_{1}h_{2} + A_{3}, \Omega_{R,suc}\right) \mathbb{P}\left((a_{s} - \gamma_{th}(1 - a_{s})) h_{3} \geq A_{4}\right), \tag{14}$$

Cases:	Outage Probability of The Primary Transmission $P_{ m out,p}$			
$0 \le a_s \le \frac{\gamma_{\rm th}}{1 + \gamma_{\rm th}}$	$P_{\text{out,p}} = 1 - P_{12} \exp\left(-\frac{A_4}{\lambda_3}\right) - \exp\left(-\frac{A_3}{\lambda_0} - \frac{A_4}{\lambda_3}\right) \left(1 - \exp\left(-\frac{A_1}{\lambda_1}\right)\right)$			
$\frac{\gamma_{\rm th}}{1+\gamma_{\rm th}} < a_s \le 1$	$P_{\rm out,p} \approx 1 - \exp\left(-\frac{A_4}{(a_s - \gamma_{\rm th}(1 - a_s))\lambda_3}\right) \left(-\theta \exp\left(\theta - \frac{A_1}{\lambda_1} - \frac{A_3}{\lambda_0}\right) \operatorname{Ei}\left(-\theta\right) - P_{12}\right) - P_{12} \exp\left(-\frac{A_4}{\lambda_3}\right)$			
	$-\exp\left(-\frac{A_3}{\lambda_0} - \frac{A_4}{\lambda_3}\right)\left(1 - \exp\left(-\frac{A_1}{\lambda_1}\right)\right)$			
where $P_{12} \approx e^{-\frac{A_1}{\lambda_1} - \frac{A_3}{\lambda_0}} \left[\frac{\pi \varpi}{2GA_5} \sum_{g=1}^G \sqrt{1 - v_g^2} e^{-\frac{A_2 \kappa_g^{(0)}}{\lambda_0}} f_{h_1 h_2} \left(\kappa_g^{(0)} \right) + \frac{\pi (\chi - \varpi)}{2GA_5} \sum_{g=1}^G \sqrt{1 - v_g^2} e^{-\frac{A_2 \kappa_g^{(1)}}{\lambda_0}} f_{h_1 h_2} \left(\kappa_g^{(1)} \right) \left(A_6 - \omega A_5 \kappa_g^{(1)} \right) \right]$				
with $A_2 = \gamma_{\mathrm{th}} \beta d_1^{-\alpha_1} d_2^{-\alpha_2} d_0^{\alpha_0}$, $A_6 = \frac{1}{2} + \omega \vartheta$ and $A_5 = \frac{\beta P_0 d_1^{-\alpha_1} d_2^{-\alpha_2}}{\sigma^2}$, $A_4 = \frac{\gamma_{\mathrm{th}} \sigma^2 d_3^{\alpha_3}}{P_{\mathrm{R}}}$, $A_3 = \frac{\gamma_{\mathrm{th}} \sigma^2 d_0^{\alpha_0}}{P_0}$, $A_1 = \frac{d_1^{\alpha_1} F_{\mathrm{NL}}^{-1}(P_{\mathrm{c}})}{F_{\mathrm{NL}}(P_{\mathrm{c}})}$ and $\theta = \frac{\lambda_0}{\lambda_1 \lambda_2 A_2}$.				

where $x=h_1,y=h_1h_2,z=h_0,f_{h_1}(x)=\frac{1}{\lambda_1}\exp\left(-\frac{x}{\lambda_1}\right),f_{h_0}(z)=\frac{1}{\lambda_0}\exp\left(-\frac{z}{\lambda_0}\right),\theta=\frac{\lambda_0}{\lambda_1\lambda_2A_2},$ step (aa) holds following Appendix C in [9] and the exponential integral function $\mathrm{Ei}(-\theta)=\int_{-\infty}^{-\theta}t^{-1}e^tdt.$

Based on (12), P_{12} can be computed as

$$P_{12} = \mathbb{P}\left(h_{1} \geq A_{1}, h_{0} \geq A_{2}h_{1}h_{2} + A_{3}, \Omega_{R, \text{fail}}\right)$$

$$= \int_{A_{1}}^{+\infty} f_{h_{1}}(x) \int_{0}^{+\infty} f_{h_{1}h_{2}}(y) \varepsilon_{R,c} \int_{A_{2}y+A_{3}}^{+\infty} (z) dz dy dx$$

$$\approx \int_{A_{1}}^{+\infty} f_{h_{1}}(x) dx \int_{0}^{+\infty} f_{h_{1}h_{2}}(y) \Psi\left(\gamma_{R,c}^{a}\right) \int_{A_{2}y+A_{3}}^{+\infty} f_{h_{0}}(z) dz dy$$

$$= e^{-\frac{A_{1}}{\lambda_{1}} - \frac{A_{3}}{\lambda_{0}}} \int_{0}^{+\infty} f_{h_{1}h_{2}}(y) e^{-\frac{A_{2}y}{\lambda_{0}}} \Psi\left(A_{5}y\right) dy, \tag{18}$$

where $A_5 = \frac{\beta P_0 d_1^{-\alpha_1} d_2^{-\alpha_2}}{\sigma^2}$.

Due to the Gaussian Q function in $\Psi(A_5y)$, it is very challenging to derive the closed-form solution of P_{12} . Following [22], [23], [32], we adopt the linearization technique to approximate $\Psi(A_5y)$ as

$$\Psi(A_5 y) \approx \begin{cases} 1, A_5 y < \varpi \\ \frac{1}{2} - \omega(A_5 y - \vartheta), \varpi \le A_5 y \le \chi \\ 0, A_5 y > \chi \end{cases}$$
(19)

where
$$\omega=\frac{\sqrt{N_c}}{\sqrt{2\pi\left(2^{\frac{2B_c}{N_c}}-1\right)}}, \vartheta=2^{\frac{B_c}{N_c}}-1, \varpi=\vartheta-\frac{1}{2\omega}$$
 and $\gamma=\vartheta+\frac{1}{2\omega}$

Based on (19), we can approximate P_{12} as

$$P_{12} \approx e^{-\frac{A_1}{\lambda_1} - \frac{A_3}{\lambda_0}} \left[\int_0^{\varpi/A_5} f_{h_1 h_2}(y) e^{-\frac{A_2 y}{\lambda_0}} dy + A_6 \int_{\varpi/A_5}^{\chi/A_5} f_{h_1 h_2}(y) \right] \times e^{-\frac{A_2 y}{\lambda_0}} dy - \omega A_5 \int_{\varpi/A_5}^{\chi/A_5} f_{h_1 h_2}(y) e^{-\frac{A_2 y}{\lambda_0}} y dy, \qquad (20)$$

where $A_6 = \frac{1}{2} + \omega \vartheta$.

Although (20) has simpler form than (18), the closed-form expression for P_{12} is still unavailable since the integrals, i.e., $\int_0^{\varpi/A_5} f_{h_1h_2}\left(y\right) e^{-\frac{A_2y}{\lambda_0}} dy$ and $\int_{\varpi/A_5}^{\chi/A_5} f_{h_1h_2}\left(y\right) e^{-\frac{A_2y}{\lambda_0}} y dy$, can

not be obtained directly. Following [9], [10], we apply Gaussian-Chebyshev quadrature to approximate P_{12} . Thus, P_{12} is approximated as

$$P_{12} \approx e^{-\frac{A_{1}}{\lambda_{1}} - \frac{A_{3}}{\lambda_{0}}} \left[\frac{\pi \varpi}{2GA_{5}} \sum_{g=1}^{G} \sqrt{1 - v_{g}^{2}} e^{-\frac{A_{2}\kappa_{g}^{(0)}}{\lambda_{0}}} f_{h_{1}h_{2}} \left(\kappa_{g}^{(0)}\right) + \frac{\pi \left(\chi - \varpi\right)}{2GA_{5}} \sum_{g=1}^{G} \sqrt{1 - v_{g}^{2}} e^{-\frac{A_{2}\kappa_{g}^{(1)}}{\lambda_{0}}} \times f_{h_{1}h_{2}} \left(\kappa_{g}^{(1)}\right) \left(A_{6} - \omega A_{5}\kappa_{g}^{(1)}\right) \right], \tag{21}$$

where $v_g=\cos\frac{2g-1}{2G}\pi$, $\kappa_g^{(0)}=\frac{\varpi}{2A_5}v_g+\frac{\varpi}{2A_5}$, $\kappa_g^{(1)}=\frac{\chi-\varpi}{2A_5}v_g+\frac{\chi+\varpi}{2A_5}$, and the parameter G decides the tradeoff between complexity and accuracy. Note that a larger G brings a more accurate expression for P_{12} , but also makes the expression more complex [10].

Based on P_{11} in (17) and P_{12} in (21), the closed-form expression of P_1 can be obtained.

B. Derivations of P_2 and P_3

According to (13), P_2 can be calculated as

$$P_{2} = \mathbb{P}(h_{1} \geq A_{1}, h_{0} \geq A_{2}h_{1}h_{2} + A_{3}, \Omega_{R, \text{fail}}, h_{3} \geq A_{4})$$

$$= P_{12}\mathbb{P}(h_{3} \geq A_{4})$$

$$\approx e^{-\frac{A_{1}}{\lambda_{1}} - \frac{A_{3}}{\lambda_{0}} - \frac{A_{4}}{\lambda_{3}}} \left[\frac{\pi \varpi}{2GA_{5}} \sum_{g=1}^{G} \sqrt{1 - v_{g}^{2}} e^{-\frac{A_{2}\kappa_{g}^{(0)}}{\lambda_{0}}} \right]$$

$$\times f_{h_{1}h_{2}} \left(\kappa_{g}^{(0)}\right) + \frac{A_{6}\pi \left(\chi - \varpi\right)}{2GA_{5}} \sum_{g=1}^{G} \sqrt{1 - v_{g}^{2}}$$

$$\times e^{-\frac{A_{2}\kappa_{g}^{(1)}}{\lambda_{0}}} f_{h_{1}h_{2}} \left(\kappa_{g}^{(1)}\right) \left(1 - \omega A_{5}\kappa_{g}^{(1)}\right) \right]. \tag{22}$$

As for P_3 , it can be calculated as

$$P_3 = \mathbb{P}(h_1 < A_1, h_0 \ge A_3, h_3 \ge A_4)$$

$$= \exp\left(-\frac{A_3}{\lambda_0} - \frac{A_4}{\lambda_3}\right) \left(1 - \exp\left(-\frac{A_1}{\lambda_1}\right)\right). \tag{23}$$

C. Expression of $P_{\text{out,p}}$

Based on the derivations of P_1, P_2 and P_3 , we can obtain the closed-form expression of $P_{\mathrm{out,p}}$ and it is summarized in Table I. As shown in Table I, there are two cases for the expression of $P_{\mathrm{out,p}}$, i.e., the case with $0 \leq a_s \leq \frac{\gamma_{\mathrm{th}}}{1+\gamma_{\mathrm{th}}}$ and the case with $\frac{\gamma_{\mathrm{th}}}{1+\gamma_{\mathrm{th}}} < a_s \leq 1$, respectively. In the case of $0 \leq a_s \leq \frac{\gamma_{\mathrm{th}}}{1+\gamma_{\mathrm{th}}}$, IR always fails to decode \widehat{s} when R successfully decodes both s and c, leading to $P_1 = 0$. Thus, $P_{\mathrm{out,p}}$ of this case is determined by $1-P_2-P_3$, where P_2 and P_3 are given by (22) and (23). In the case of $\frac{\gamma_{\mathrm{th}}}{1+\gamma_{\mathrm{th}}} < a_s \leq 1$, $P_{\mathrm{out,p}}$ is given by $1-P_1-P_2-P_3$, where P_1 is achieved by (15), (17) and (21). It can be observed that $P_{\mathrm{out,p}}$ in the case with $0 \leq a_s \leq \frac{\gamma_{\mathrm{th}}}{1+\gamma_{\mathrm{th}}}$ is always higher than that in the case with $\frac{\gamma_{\mathrm{th}}}{1+\gamma_{\mathrm{th}}} < a_s \leq 1$. This indicates that when R decodes both s and c successfully, $a_s > \frac{\gamma_{\mathrm{th}}}{1+\gamma_{\mathrm{th}}}$ should be guaranteed to achieve a lower outage probability for the primary transmission.

IV. PERFORMANCE ANALYSIS FOR AMBACKCOM

In this section, we aim to analyze the average BLER of AmBackCom. The average BLER of AmBackCom, denoted by $\varepsilon_{\rm BL}$, is the probability of AmBackCom experiencing a block error averaged over the fading channels. In order to achieve a successful transmission for AmBackCom, BT should harvest enough energy to support AmBackCom, and both R and IR should decode the long-packet information and the short-packet information successfully. Taking both the energy causality constraint at BT and the decoding error of SIC into account, $\varepsilon_{\rm BL}$ is given by

$$\varepsilon_{\text{BL}} = 1 - \mathbb{P}\left(E_{\text{BT}} \ge \frac{P_{\text{c}}T}{2}, \gamma_{\text{R},s}^{\text{a}} \ge \gamma_{\text{th}}, \Omega_{\text{R,suc}}, \gamma_{\text{IR},s}^{\text{I}} \ge \gamma_{\text{th}}, \Omega_{\text{IR,suc}}\right)$$

$$= 1 - \underbrace{\mathbb{P}\left(h_1 \ge A_1, h_0 \ge A_2 h_1 h_2 + A_3, \Omega_{\text{R,suc}}\right)}_{P_4} \times \underbrace{\mathbb{P}\left(\left(a_s - \gamma_{\text{th}} \left(1 - a_s\right)\right) h_3 \ge A_4, \Omega_{\text{IR,suc}}\right)}_{P_5}, \tag{24}$$

where $\Omega_{\mathrm{IR,suc}}$ refers to the event that IR can decode \widehat{c} successfully and happens under given $\gamma_{\mathrm{IR},c}^{\mathrm{I}}$ with the probability $1-\varepsilon_{\mathrm{IR},c}$. Note that the closed-form expression for $\varepsilon_{\mathrm{BL}}$ is hard to achieve due to the coupled relationships among E_{BT} , $\gamma_{\mathrm{R},s}^{\mathrm{a}}$, and $\Omega_{\mathrm{R,suc}}$.

Based on (24), we can find that when $a_s - \gamma_{\rm th} \, (1-a_s) \leq 0$, i.e., $0 \leq a_s \leq \frac{\gamma_{\rm th}}{1+\gamma_{\rm th}}$, holds, P_5 is always 0 and thus we have $\varepsilon_{\rm BL} = 1$. When $a_s - \gamma_{\rm th} \, (1-a_s) > 0$, i.e., $\frac{\gamma_{\rm th}}{1+\gamma_{\rm th}} < a_s \leq 1$, $\varepsilon_{\rm BL}$ can be obtained after resolving P_4 and P_5 .

As for P_4 , it can be calculated as

$$P_4 = \mathbb{P}(h_1 \ge A_1, h_0 \ge A_2 h_1 h_2 + A_3, \Omega_{\text{R,suc}})$$

= $P_{11} - P_{12}$, (25)

where $P_{11} = \mathbb{P}(h_1 \geq A_1, h_0 \geq A_2 h_1 h_2 + A_3)$ is given in (17) and $P_{12} = \mathbb{P}(h_1 \geq A_1, h_0 \geq A_2 h_1 h_2 + A_3, \Omega_{R,fail})$ can be approximated as (21).

Then P_5 can be rewritten as

$$P_{5} = \mathbb{P}\left(\left(a_{s} - \gamma_{\text{th}}\left(1 - a_{s}\right)\right) h_{3} \ge A_{4}\right) - P_{51}$$

$$= \exp\left(-\frac{A_{4}}{\left(a_{s} - \gamma_{\text{th}}\left(1 - a_{s}\right)\right) \lambda_{3}}\right) - P_{51}, \qquad (26)$$

where $P_{51} = \mathbb{P}\left(\left(a_s - \gamma_{\rm th}\left(1 - a_s\right)\right) h_3 \geq A_4, \Omega_{\rm IR,fail}\right)$. Based on (12), P_{51} can be calculated as

$$P_{51} = \int_{\frac{A_4}{a_s - \gamma_{\text{th}}(1 - a_s)}}^{+\infty} \varepsilon_{\text{IR},c} f_{h_3} (v) dv$$

$$\approx \int_{\frac{A_4}{a_s - \gamma_{\text{th}}(1 - a_s)}}^{+\infty} \Psi (A_7 v) f_{h_3} (v) dv \qquad (27)$$

where $v = h_3$, $f_{h_3}(v) = \frac{1}{\lambda_3} \exp\left(-\frac{v}{\lambda_3}\right)$ and $A_7 = \frac{(1-a_s)P_{\rm R}d_3^{-\alpha_3}}{2}$.

Similar to P_{12} , the linearization technique is adopted. By comparing $\frac{A_4}{a_s-\gamma_{\rm th}(1-a_s)}$ with $\frac{\varpi}{A_7}$ and $\frac{\chi}{A_7}$, there are three cases for the value of P_{51} , which are the case with $\frac{A_4}{a_s-\gamma_{\rm th}(1-a_s)}<\frac{\varpi}{A_7}$, the case with $\frac{\varpi}{A_7}\leq\frac{A_4}{a_s-\gamma_{\rm th}(1-a_s)}\leq\frac{\chi}{A_7}$, and the case with $\frac{A_4}{a_s-\gamma_{\rm th}(1-a_s)}>\frac{\chi}{A_7}$, respectively. Specifically, for the case with $\frac{A_4}{a_s-\gamma_{\rm th}(1-a_s)}<\frac{\varpi}{A_7}$, P_{51} is determined by

$$P_{51} \approx \int_{\frac{A_4}{a_s - \gamma_{\text{th}}(1 - a_s)}}^{\frac{\varpi}{A_7}} f_{h_3}(v) dv + \int_{\frac{\varpi}{A_7}}^{\frac{\chi}{A_7}} \left[\frac{1}{2} - \omega \left(A_7 v - \vartheta \right) \right] f_{h_3}(v) dv$$

$$\approx \exp \left(-\frac{A_4}{\left(a_s - \gamma_{\text{th}} \left(1 - a_s \right) \right) \lambda_3} \right) + \lambda_3 A_7 \omega$$

$$\times \left(\exp \left(-\frac{\chi}{A_7 \lambda_3} \right) - \exp \left(-\frac{\varpi}{A_7 \lambda_3} \right) \right). \tag{28}$$

For the case with $\frac{\varpi}{A_7} \leq \frac{A_4}{a_s - \gamma_{\rm th}(1-a_s)} \leq \frac{\chi}{A_7}$, P_{51} can be calculated as

$$P_{51} \approx \int_{\frac{A_4}{a_s - \gamma_{\text{th}}(1 - a_s)}}^{\frac{\chi}{A_7}} \left[\frac{1}{2} - \omega \left(A_7 v - \vartheta \right) \right] f_{h_3}(v) \, dv$$

$$\approx \exp \left(-\frac{A_4}{\left(a_s - \gamma_{\text{th}} \left(1 - a_s \right) \right) \lambda_3} \right) \left(\frac{1}{2} + \omega \vartheta - \lambda_3 A_7 \omega \right)$$

$$-\frac{A_4 \omega A_7}{a_s - \gamma_{\text{th}} \left(1 - a_s \right)} + \lambda_3 \omega A_7 \exp \left(-\frac{\chi}{A_7 \lambda_3} \right). \tag{29}$$

For the case with $\frac{A_4}{a_s-\gamma_{\rm th}(1-a_s)}>\frac{\chi}{A_7},\,P_{51}$ can be approximated as $P_{51}\approx 0$.

Therefore, the closed-form expression of $\varepsilon_{\rm BL}$ can be obtained and is summarized in Table II, as shown at the top of the next page. As shown in this table, we can find that there are four cases for the expression of $\varepsilon_{\rm BL}$, which are the case with $0 \le a_s \le \frac{\gamma_{\rm th}}{1+\gamma_{\rm th}}$, the case with $\frac{\gamma_{\rm th}}{1+\gamma_{\rm th}} < a_s \le 1$ and $\frac{A_4}{a_s-\gamma_{\rm th}(1-a_s)} < \frac{\varpi}{A_7}$, the case with $\frac{\gamma_{\rm th}}{1+\gamma_{\rm th}} < a_s \le 1$ and $\frac{\varpi}{a_s-\gamma_{\rm th}(1-a_s)} \le \frac{\chi}{A_7}$, and the case with $\frac{\gamma_{\rm th}}{1+\gamma_{\rm th}} < a_s \le 1$ and $\frac{A_4}{a_s-\gamma_{\rm th}(1-a_s)} > \frac{\chi}{A_7}$, respectively. It is worth noting that when $0 \le a_s \le \frac{\gamma_{\rm th}}{1+\gamma_{\rm th}}$ holds, \hat{c} is always decoded unsuccessfully due to the failed decoding of \hat{s} based on the used SIC decoding scheme, leading to $\varepsilon_{\rm BL}=1$.

V. IMPROVED SIC DECODING SCHEME AT IR AND PERFORMANCE ANALYSIS

Based on Table I and Table II, it can be easily observed that for the case with $0 \le a_s \le \frac{\gamma_{\rm th}}{1+\gamma_{\rm th}}$, both $P_{\rm out,p}$ and $\varepsilon_{\rm BL}$ are greater than those under the case with $\frac{\gamma_{\rm th}}{1+\gamma_{\rm th}} < a_s \le 1$. In order to reduce $P_{\rm out,p}$ and $\varepsilon_{\rm BL}$ under the case with

TABLE II AVERAGE BLER OF AMBACKCOM

Cases:		Average BLER of AmBackCom $arepsilon_{ m BL}$		
$0 \le a_s \le \frac{\gamma_{ m th}}{1 + \gamma_{ m th}}$		$arepsilon_{ m BL}=1$		
	$\frac{A_4}{a_s - \gamma_{\rm th}(1 - a_s)} < \frac{\varpi}{A_7}$	$ \varepsilon_{\rm BL} \approx 1 - \lambda_3 A_7 \omega \left(\theta e^{\theta - \frac{A_1}{\lambda_1} - \frac{A_3}{\lambda_0}} \operatorname{Ei} \left(-\theta \right) + P_{12} \right) \left(\exp \left(-\frac{\chi}{A_7 \lambda_3} \right) - \exp \left(-\frac{\varpi}{A_7 \lambda_3} \right) \right) $		
	$\frac{\varpi}{A_7} \le \frac{A_4}{a_s - \gamma_{\text{th}}(1 - a_s)} \le \frac{\chi}{A_7}$	$\varepsilon_{\rm BL} \approx 1 - \left(-\theta e^{\theta - \frac{A_1}{\lambda_1} - \frac{A_3}{\lambda_0}} \operatorname{Ei}(-\theta) - P_{12}\right) \left(e^{-\frac{A_4}{(a_s - \gamma_{\rm th}(1 - a_s))\lambda_3}} - e^{-\frac{A_4}{(a_s - \gamma_{\rm th}(1 - a_s))\lambda_3}} (0.5 + \omega \vartheta - \lambda_3 A_7 \omega - \frac{A_4 \omega A_7}{a_s - \gamma_{\rm th}(1 - a_s)}\right)$		
$\frac{\gamma_{\rm th}}{1 + \gamma_{\rm th}} < a_s \le 1$		$-\lambda_3 \omega A_7 e^{-\frac{X}{A_7 \lambda_3}}$		
	$\frac{A_4}{a_s - \gamma_{\rm th}(1 - a_s)} > \frac{\chi}{A_7}$	$\varepsilon_{\rm BL} \approx 1 - \left(-\theta e^{\theta - \frac{A_1}{\lambda_1} - \frac{A_3}{\lambda_0}} \operatorname{Ei}\left(-\theta\right) - P_{12}\right) e^{-\frac{A_4}{(a_s - \gamma_{\rm th}(1 - a_s))\lambda_3}}$		
where $P_{12}, A_1, A_2, A_3, A_4, A_5, A_6$ and θ are obtained by referring to Table I, and $A_7 = \frac{(1-a_s)P_{\rm R}d_3^{-\alpha_3}}{\sigma^2}$.				

 $0 \leq a_s \leq \frac{\gamma_{\rm th}}{1+\gamma_{\rm th}}$, we propose an improved SIC decoding scheme at IR that can be detailed as following: IR first decodes \widehat{c} if $0 \leq a_s \leq \frac{\gamma_{\rm th}}{1+\gamma_{\rm th}}$; otherwise, \widehat{s} is first decoded. In what follows, we re-calculate both the outage probability of the primary transmission and the average BLER of AmBackCom, which will show the superior gain brought by the proposed SIC decoding scheme.

With the improved SIC decoding scheme considered at IR, there are two subcases for Case I, i.e., $0 \le a_s \le \frac{\gamma_{\rm th}}{1+\gamma_{\rm th}}$ and $\frac{\gamma_{\rm th}}{1+\gamma_{\rm th}} < a_s \le 1$. Specifically, for the subcase with $0 \le a_s \le \frac{\gamma_{\rm th}}{1+\gamma_{\rm th}}$, IR first decodes \hat{c} and then decodes \hat{s} after cancelling $\sqrt{(1-a_s)\,P_{\rm R}h_3d_3^{-\alpha_3}}\hat{c}$. Based on this, the SINR for decoding \hat{c} is given by

$$\gamma_{\text{IR},c}^{\text{I,F}} = \frac{(1 - a_s) P_{\text{R}} h_3 d_3^{-\alpha_3}}{a_s P_{\text{R}} h_3 d_3^{-\alpha_3} + \sigma^2},\tag{30}$$

where the superscript 'F' denotes the improved SIC decoding scheme.

If IR can successfully decode \hat{c} and then remove the interference signal $\sqrt{(1-a_s)\,P_{\rm R}h_3d_3^{-\alpha_3}}\hat{c}$ via SIC, then the decoding SNR of \hat{s} is given by

$$\gamma_{\text{IR},s}^{\text{I,F}} = \frac{a_s P_{\text{R}} h_3 d_3^{-\alpha_3}}{\sigma^2}.$$
 (31)

Note that in the subcase with $\frac{\gamma_{\rm th}}{1+\gamma_{\rm th}} < a_s \leq 1$, the SIC decoding order is the same as that in Section II and the SINR or SNR for decoding \hat{s} or \hat{c} is $\gamma_{{\rm IR},s}^{\rm I}$ or $\gamma_{{\rm IR},c}^{\rm I}$.

A. Derivation of $P_{\text{out,p}}^{\text{F}}$

Let $P_{\text{out,p}}^{\text{F}}$ denote the outage probability of the primary transmission under the improved SIC decoding scheme at IR. Then $P_{\text{out,p}}^{\text{F}}$ can be calculated as

$$P_{\text{out, p}}^{\text{F}} = 1 - P_6 - P_2 - P_3, \tag{32}$$

where P_6 is the successful transmission probability of the primary transmission in Case I under the improved SIC

decoding scheme. Accordingly, P_6 can be calculated as

$$P_{6} = \begin{cases} \mathbb{P}\left(E_{\mathrm{BT}} \geq \frac{P_{\mathrm{c}}T}{2}, \gamma_{\mathrm{R},s}^{\mathrm{a}} \geq \gamma_{\mathrm{th}}, \Omega_{\mathrm{R,suc}}, \Omega_{\mathrm{IR,suc}}^{\mathrm{F}}, \\ \gamma_{\mathrm{IR},s}^{\mathrm{I,F}} \geq \gamma_{\mathrm{th}}\right), & \text{if } 0 \leq a_{s} \leq \frac{\gamma_{\mathrm{th}}}{1+\gamma_{\mathrm{th}}}, \\ \mathbb{P}\left(E_{\mathrm{BT}} \geq \frac{P_{\mathrm{c}}T}{2}, \gamma_{\mathrm{R,s}}^{\mathrm{a}} \geq \gamma_{\mathrm{th}}, \Omega_{\mathrm{R,suc}}, \\ \gamma_{\mathrm{IR,s}}^{\mathrm{I}} \geq \gamma_{\mathrm{th}}\right), & \text{if } \frac{\gamma_{\mathrm{th}}}{1+\gamma_{\mathrm{th}}} < a_{s} \leq 1, \end{cases}$$
(33)

where $\Omega_{\rm IR,suc}^{\rm F}$ denotes the event that IR decodes \hat{c} successfully under the improved SIC decoding scheme.

Similar to the derivation of P_1 , we can obtain P_6 under the subcase with $\frac{\gamma_{\rm th}}{1+\gamma_{\rm th}} < a_s \leq 1$ as $\exp\left(-\frac{A_4}{(a_s-\gamma_{\rm th}(1-a_s))\lambda_3}\right)(P_{11}-P_{12})$, where P_{11} and P_{12} are determined by (17) and (20), respectively. As for the subcase with $0 \leq a_s \leq \frac{\gamma_{\rm th}}{1+\gamma_{\rm th}}$, P_6 can be derived as

$$\begin{split} &P_{6} = \\ &\mathbb{P}\left(E_{\text{BT}} \geq \frac{P_{\text{c}}T}{2}, \gamma_{\text{R},s}^{\text{a}} \geq \gamma_{\text{th}}, \Omega_{\text{R,suc}}, \Omega_{\text{IR,suc}}^{\text{F}}, \gamma_{\text{IR,s}}^{\text{I,F}} \geq \gamma_{\text{th}}\right) \\ &= \mathbb{P}(h_{1} \geq A_{1}, h_{0} \geq A_{2}h_{1}h_{2} + A_{3}, \Omega_{\text{R,suc}})\mathbb{P}\left(\Omega_{\text{IR,suc}}^{\text{F}}, h_{3} \geq \frac{A_{4}}{a_{s}}\right) \\ &= (P_{11} - P_{12})\left(e^{-\frac{A_{4}}{a_{s}\lambda_{3}}} - P_{61}\right), \end{split} \tag{34}$$

where $P_{61} = \mathbb{P}\left(\Omega_{\mathrm{IR,fail}}^{\mathrm{F}}, h_3 \geq \frac{A_4}{a_s}\right)$ and $\Omega_{\mathrm{IR,fail}}^{\mathrm{F}}$ denotes the event that IR fails to decode \hat{c} under the improved SIC decoding scheme.

Let $\varepsilon_{\mathrm{IR},c}^{\mathrm{F}}$ denote the probability that $\Omega_{\mathrm{IR},\mathrm{fail}}^{\mathrm{F}}$ happens under given $\gamma_{\mathrm{IR},c}^{\mathrm{I,F}}$, which can be approximated as $\Psi\left(\gamma_{\mathrm{IR},c}^{\mathrm{I,F}}\right)$. Then, P_{61} is given by

$$P_{61} = \int_{\frac{A_4}{a_s}}^{+\infty} \varepsilon_{\text{IR},c}^{\text{F}} f_{h_3}(v) dv$$

$$\approx \int_{\frac{A_4}{a_s}}^{+\infty} \Psi\left(\gamma_{\text{IR},c}^{\text{I,F}}\right) f_{h_3}(v) dv$$

$$= \int_{\frac{A_4}{a_s}}^{+\infty} \Psi\left(\frac{(1-a_s) P_{\text{R}} v d_3^{-\alpha_3}}{a_s P_{\text{R}} v d_3^{-\alpha_3} + \sigma^2}\right) f_{h_3}(v) dv \qquad (35)$$

Since $h_3 \geq \frac{A_4}{a_s}$, we can obtain the range of $\gamma_{{\rm IR},c}^{{
m I},{
m F}}$, given by

$$\frac{(1-a_s)\gamma_{\rm th}}{a_s(\gamma_{\rm th}+1)} \le \gamma_{\rm IR,c}^{\rm I,F} = \frac{(1-a_s)P_{\rm R}h_3d_3^{-\alpha_3}}{a_sP_{\rm R}h_3d_3^{-\alpha_3} + \sigma^2} \le \frac{1-a_s}{a_s}.$$
 (36)

Based on (19), there are six cases for the expression of P_{61} by comparing the range of $\gamma_{\mathrm{IR},c}^{\mathrm{I,F}}$ with ϖ and χ .

Case 1: When $\frac{1-a_s}{a_s} \le \overline{\omega}$ is satisfied, we can obtain $\Psi\left(\gamma_{{\rm IR},c}^{{
m I,F}}\right)pprox 1$ in the range of $h_3.$ Accordingly, P_{61} in this case is given by

$$P_{61} \approx \int_{\frac{A_4}{a_{cs}}}^{+\infty} f_{h_3}(v) dv = \exp\left(-\frac{A_4}{a_s \lambda_3}\right). \tag{37}$$

Case 2: When $\frac{(1-a_s)\gamma_{\rm th}}{a_s(\gamma_{\rm th}+1)} \leq \varpi \leq \frac{1-a_s}{a_s} \leq \chi$ holds, we can obtain $\Psi\left(\gamma_{\rm IR,c}^{\rm I,F}\right) \approx 1$ with $\frac{A_4}{a_s} \leq h_3 \leq A_8$ and $\Psi\left(\gamma_{\mathrm{IR},c}^{\mathrm{I,F}}\right) \approx \frac{1}{2} - \omega\left(\gamma_{\mathrm{IR},c}^{\mathrm{I,F}} - \vartheta\right)$ with $h_3 > A_8$, where $A_8 = \frac{\varpi\sigma^2 d_3^{\alpha_3}}{P_{\mathrm{R}}(1 - a_s - \varpi a_s)}$. Thus, P_{61} in this case is given by

$$P_{61} \approx \int_{\frac{A_4}{a_s}}^{A_8} f_{h_3}(v) \, dv + \left(\frac{1}{2} + \vartheta \omega\right) \int_{A_8}^{+\infty} f_{h_3}(v) \, dv$$

$$- \omega \int_{A_8}^{+\infty} \frac{(1 - a_s) P_R v d_3^{-\alpha_3}}{a_s P_R v d_3^{-\alpha_3} + \sigma^2} f_{h_3}(v) \, dv$$

$$\approx e^{-\frac{A_4}{a_s \lambda_3}} + \left(\vartheta \omega - \frac{1}{2}\right) e^{-\frac{A_8}{\lambda_3}} - \frac{\omega(1 - a_s)}{a_s}$$

$$\times \left(e^{-\frac{A_8}{\lambda_3}} + \frac{A_9}{\lambda_3} e^{\frac{A_9}{\lambda_3}} \operatorname{Ei}\left(-\frac{A_8 + A_9}{\lambda_3}\right)\right), \quad (38)$$

where $A_9 = \frac{\sigma^2 d_3^{\alpha_3}}{a_s P_{\mathrm{R}}}$. Case 3: When $\varpi \leq \frac{(1-a_s)\gamma_{\mathrm{th}}}{a_s(\gamma_{\mathrm{th}}+1)} \leq \frac{1-a_s}{a_s} \leq \chi$ holds, we have $\Psi\left(\gamma_{\mathrm{IR},c}^{\mathrm{I,F}}\right) \approx \frac{1}{2} - \omega\left(\gamma_{\mathrm{IR},c}^{\mathrm{I,F}} - \vartheta\right)$ with any given h_3 . Correspondingly, P_{61} in this case can be computed as

$$P_{61} \approx \left(\frac{1}{2} + \vartheta\omega - \frac{\omega \left(1 - a_s\right)}{a_s}\right) e^{-\frac{A_4}{a_s \lambda_3}}$$
$$-\frac{\omega \left(1 - a_s\right) A_9}{a_s \lambda_3} e^{\frac{A_9}{\lambda_3}} \operatorname{Ei}\left(-\frac{A_4 + A_9 a_s}{\lambda_3 a_s}\right). \tag{39}$$

Case 4: If $\varpi \leq \frac{(1-a_s)\gamma_{\rm th}}{a_s(\gamma_{\rm th}+1)} \leq \chi \leq \frac{1-a_s}{a_s}$ holds, then there are two expressions to approximate $\Psi\left(\gamma_{\mathrm{IR},c}^{\mathrm{I,F}}\right)$, which are
$$\begin{split} &\Psi\left(\gamma_{\mathrm{IR},c}^{\mathrm{I,F}}\right)\approx\frac{1}{2}-\omega\left(\gamma_{\mathrm{IR},c}^{\mathrm{I,F}}-\vartheta\right) \text{ with } \frac{A_4}{a_s}\leq h_3\leq A_{10} \text{ and } \\ &A_{10}=\frac{\chi\sigma^2d_3^{\alpha_3}}{P_{\mathrm{R}}(1-a_s-\chi a_s)}, \text{ and } \Psi\left(\gamma_{\mathrm{IR},c}^{\mathrm{I,F}}\right)\approx 0 \text{ with } h_3>A_{10}. \text{ In this case, } P_{61} \text{ can be approximated as} \end{split}$$

$$P_{61} \approx \left(\frac{1}{2} + \vartheta\omega - \frac{\omega\left(1 - a_{s}\right)}{a_{s}}\right) \left(e^{-\frac{A_{4}}{a_{s}\lambda_{3}}} - e^{-\frac{A_{10}}{\lambda_{3}}}\right) + \left(\operatorname{Ei}\left(-\frac{A_{10} + A_{9}}{\lambda_{3}}\right) - \operatorname{Ei}\left(-\frac{A_{4} + A_{9}a_{s}}{\lambda_{3}a_{s}}\right)\right) \times \frac{\omega\left(1 - a_{s}\right)A_{9}e^{\frac{A_{9}}{\lambda_{3}}}}{a_{s}\lambda_{2}}.$$

$$(40)$$

Case 5: If $\frac{(1-a_s)\gamma_{\rm th}}{a_s(\gamma_{\rm th}+1)} \le \varpi \le \chi \le \frac{1-a_s}{a_s}$ is satisfied, then there are three expressions for approximating $\Psi\left(\gamma_{\mathrm{IR},c}^{\mathrm{I,F}}\right)$. Specifically, with $\frac{A_4}{a_s} \leq h_3 \leq A_8$, we have $\Psi\left(\gamma_{\text{IR},c}^{\text{I,F}}\right) \approx 1$. With $A_8 < h_3 \le A_{10}$, $\Psi\left(\gamma_{\mathrm{IR},c}^{\mathrm{I,F}}\right)$ is approximated as $\frac{1}{2} - \omega\left(\gamma_{\mathrm{IR},c}^{\mathrm{I,F}} - \vartheta\right)$ and $\Psi\left(\gamma_{\mathrm{IR},c}^{\mathrm{I,F}}\right) \approx 0$ holds for $h_3 > A_{10}$. Accordingly, P_{61} of this case is determined by

$$P_{61} \approx e^{-\frac{A_4}{a_s \lambda_3}} + \left(\frac{1}{2} + \vartheta\omega - \frac{\omega (1 - a_s)}{a_s}\right)$$

$$\times \left(e^{-\frac{A_8}{\lambda_3}} - e^{-\frac{A_{10}}{\lambda_3}}\right) - e^{-\frac{A_8}{\lambda_3}} + \frac{\omega (1 - a_s) A_9 e^{\frac{A_9}{\lambda_3}}}{a_s \lambda_3}$$

$$\times \left(\text{Ei}\left(-\frac{A_{10} + A_9}{\lambda_3}\right) - \text{Ei}\left(-\frac{A_8 + A_9}{\lambda_3}\right)\right). \tag{41}$$

Case 6: If $\chi \leq \frac{(1-a_s)\gamma_{\rm th}}{a_s(\gamma_{\rm th}+1)} \leq \frac{1-a_s}{a_s}$ holds, then $\Psi\left(\gamma_{{\rm IR},c}^{{\rm I},{\rm F}}\right) \approx 0$ holds for any given h_3 . In this case, $P_{61} \approx 0$.

Based on the above six cases, we can obtain the expression of $P_{\text{out,p}}^{\text{F}}$

B. Derivation of $\varepsilon_{\rm BL}^{\rm F}$

Let $\varepsilon_{\mathrm{BL}}^{\mathrm{F}}$ denote the average BLER of AmBackCom under the improved SIC decoding scheme at IR, and it can be

$$\varepsilon_{\mathrm{BL}}^{\mathrm{F}} = \begin{cases} & 1 - \mathbb{P}\left(E_{\mathrm{BT}} \geq \frac{P_{\mathrm{c}}T}{2}, \gamma_{\mathrm{R},s}^{\mathrm{a}} \geq \gamma_{\mathrm{th}}, \Omega_{\mathrm{R,suc}}, \Omega_{\mathrm{IR,suc}}^{\mathrm{F}}\right), \\ & \text{if } 0 \leq a_{s} \leq \frac{\gamma_{\mathrm{th}}}{1 + \gamma_{\mathrm{th}}}, \\ & 1 - (P_{11} - P_{12}) \left(e^{-\frac{A_{4}}{(a_{s} - \gamma_{\mathrm{th}}(1 - a_{s}))\lambda_{3}} - P_{51}\right), \\ & \text{if } \frac{\gamma_{\mathrm{th}}}{1 + \gamma_{\mathrm{th}}} < a_{s} \leq 1. \end{cases}$$

$$(42)$$

Let $P_7 = \mathbb{P}\left(E_{\mathrm{BT}} \geq \frac{P_{\mathrm{c}}T}{2}, \gamma_{\mathrm{R},s}^{\mathrm{a}} \geq \gamma_{\mathrm{th}}, \Omega_{\mathrm{R,suc}}, \Omega_{\mathrm{IR,suc}}^{\mathrm{F}}\right)$ then we have

$$P_{7} = \mathbb{P}\left(E_{\mathrm{BT}} \ge \frac{P_{\mathrm{c}}T}{2}, \gamma_{\mathrm{R},s}^{\mathrm{a}} \ge \gamma_{\mathrm{th}}, \Omega_{\mathrm{R,suc}}\right) \left(1 - \mathbb{P}\left(\Omega_{\mathrm{IR,fail}}^{\mathrm{F}}\right)\right)$$

$$= \left(P_{11} - P_{12}\right) \left(1 - P_{71}\right), \tag{43}$$

where $P_{71} = \mathbb{P}\left(\Omega_{\mathrm{IR,fail}}^{\mathrm{F}}\right)$. Based on the expression of $\gamma_{\mathrm{IR},c}^{\mathrm{I,F}}$, we can calculate P_{71} as

$$P_{71} = \int_{0}^{+\infty} \varepsilon_{\text{IR},c}^{\text{F}} f_{h_3}(v) \, dv$$

$$\approx \int_{0}^{+\infty} \Psi\left(\gamma_{\text{IR},c}^{\text{I,F}}\right) f_{h_3}(v) \, dv. \tag{44}$$

Since the range of $\gamma_{{\rm IR},c}^{{\rm I,F}}$ is given by $0 \leq \gamma_{{\rm IR},c}^{{\rm I,F}} =$ $\frac{(1-a_s)P_{\rm R}h_3d_3^{-\alpha_3}}{a_sP_{\rm R}h_3d_3^{-\alpha_3}+\sigma^2} \leq \frac{1-a_s}{a_s}, \text{ there are three cases for the expression of } P_{71} \text{ by comparing } \frac{1-a_s}{a_s} \text{ with } \varpi \text{ and } \chi.$

Specifically, for the case with $\frac{1-a_s}{a_s} \leq \varpi$, $\Psi\left(\gamma_{\mathrm{IR},c}^{\mathrm{I,F}}\right) \approx 1$ always holds. Then P_{71} can be computed as

$$P_{71} \approx \int_0^{+\infty} f_{h_3}(v) dv = 1. \tag{45}$$

In this case, we can obtain $\varepsilon_{\mathrm{BL}}^{\mathrm{F}} \approx 1$. For the case with $\varpi \leq \frac{1-a_s}{a_s} \leq \chi$, there are two expressions to approximate $\Psi\left(\gamma_{\mathrm{IR},c}^{\mathrm{I,F}}\right)$, which are $\Psi\left(\gamma_{\mathrm{IR},c}^{\mathrm{I,F}}\right) \approx 1$ for $0 \leq$ $h_3 \leq A_8$ and $\Psi\left(\gamma_{\mathrm{IR},c}^{\mathrm{I,F}}\right) \approx \frac{1}{2} - \omega\left(\gamma_{\mathrm{IR},c}^{\mathrm{I,F}} - \vartheta\right)$ with $h_3 > A_8$. In this case, P_{71} is given by

$$P_{71} \approx 1 + \left(\omega \vartheta - \frac{1}{2}\right) e^{-\frac{A_8}{\lambda_3}} - \frac{\omega \left(1 - a_s\right)}{a_s} \times \left(e^{-\frac{A_8}{\lambda_3}} + \frac{A_9}{\lambda_3} e^{\frac{A_9}{\lambda_3}} \operatorname{Ei}\left(-\frac{A_8 + A_9}{\lambda_3}\right)\right). \tag{46}$$

TABLE III SUMMARY OF $P_{\mathrm{out,p}}^{\mathrm{F}}$ and $\varepsilon_{\mathrm{BL}}^{\mathrm{F}}$

Cases:	$P^{ m F}_{ m out,p}$	$arepsilon_{ m BL}^{ m F}$
$\frac{1-a_s}{a_s} \le \varpi$	$P_{\text{out,p}}^{\text{F}} \approx 1 - P_{12}e^{-\frac{A_4}{\lambda_3}} - e^{-\frac{A_3}{\lambda_0} - \frac{A_4}{\lambda_3}} \left(1 - e^{-\frac{A_1}{\lambda_1}}\right)$	$\varepsilon_{\mathrm{BL}}^{\mathrm{F}} \approx 1$
$\frac{(1-a_s)\gamma_{th}}{a_s(\gamma_{th}+1)} \le \varpi$ $\le \frac{1-a_s}{a_s} \le \chi$	$P_{\text{out,p}}^{\text{F}} \approx 1 - P_{12}e^{-\frac{A_4}{\lambda_3}} - e^{-\frac{A_3}{\lambda_0} - \frac{A_4}{\lambda_3}} \left(1 - e^{-\frac{A_1}{\lambda_1}}\right)$ $+ \left(\theta e^{\theta - \frac{A_1}{\lambda_1} - \frac{A_3}{\lambda_0}} \operatorname{Ei}\left(-\theta\right) + P_{12}\right) \left(\frac{\omega(1 - a_s)}{a_s}\right)$ $\times \left(e^{-\frac{A_8}{\lambda_3}} + \frac{A_9}{\lambda_3} e^{\frac{A_9}{\lambda_3}} \operatorname{Ei}\left(-\frac{A_8 + A_9}{\lambda_3}\right)\right)$ $- (\vartheta \omega - 0.5) e^{-\frac{A_8}{\lambda_3}}$	$\varepsilon_{\rm BL}^{\rm F} \approx 1 + \left(\theta e^{\theta - \frac{A_1}{\lambda_1} - \frac{A_3}{\lambda_0}} \operatorname{Ei}(-\theta) + P_{12}\right)$ $\times \left(\frac{\omega(1 - a_s)}{a_s} \left(\operatorname{Ei}\left(-\frac{A_8 + A_9}{\lambda_3}\right) \frac{A_9}{\lambda_3} e^{\frac{A_9}{\lambda_3}}\right) + e^{-\frac{A_8}{\lambda_3}} \left(\omega \vartheta - 0.5\right)\right)$
$\varpi \le \frac{(1 - a_s)\gamma_{\text{th}}}{a_s(\gamma_{\text{th}} + 1)}$ $\le \frac{1 - a_s}{a_s} \le \chi$	$P_{\text{out,p}}^{\text{F}} \approx 1 - P_{12}e^{-\frac{A_4}{\lambda_3}} - e^{-\frac{A_3}{\lambda_0} - \frac{A_4}{\lambda_3}} \left(1 - e^{-\frac{A_1}{\lambda_1}}\right) + \left(\theta e^{\theta - \frac{A_1}{\lambda_1} - \frac{A_3}{\lambda_0}} \text{Ei}\left(-\theta\right) + P_{12}\right) \left(\text{Ei}\left(-\frac{A_4 + A_9 a_s}{\lambda_3 a_s}\right) \times \frac{\omega(1 - a_s) A_9}{a_s \lambda_3} e^{\frac{A_9}{\lambda_3}} + e^{-\frac{A_4}{a_s \lambda_3}} \left(\frac{1}{2} - \vartheta \omega + \frac{\omega(1 - a_s)}{a_s}\right)\right)$	TE 3) - E 3 (WV - 0.5))
$0 \le a_s \qquad \qquad \varpi \le \frac{(1 - a_s)\gamma_{\text{th}}}{a_s(\gamma_{\text{th}} + 1)}$ $\le \frac{\gamma_{\text{th}}}{1 + \gamma_{\text{th}}} \qquad \le \chi \le \frac{1 - a_s}{a_s}$	$P_{\text{out,p}}^{\text{F}} \approx 1 - P_{12}e^{-\frac{A_4}{\lambda_3}} - e^{-\frac{A_3}{\lambda_0} - \frac{A_4}{\lambda_3}} \left(1 - e^{-\frac{A_1}{\lambda_1}}\right)$ $+ \left(\theta e^{\theta - \frac{A_1}{\lambda_1} - \frac{A_3}{\lambda_0}} \operatorname{Ei}\left(-\theta\right) + P_{12}\right) \left(e^{-\frac{A_4}{a_s \lambda_3}} - \left(\frac{1}{2}\right)\right)$ $+ \vartheta \omega - \frac{\omega(1 - a_s)}{a_s} \left(e^{-\frac{A_4}{a_s \lambda_3}} - e^{-\frac{A_{10}}{\lambda_3}}\right)$ $- \left(\operatorname{Ei}\left(-\frac{A_{10} + A_9}{\lambda_3}\right) - \operatorname{Ei}\left(-\frac{A_4 + A_9 a_s}{\lambda_3 a_s}\right)\right)$ $\times \frac{\omega(1 - a_s) A_9 e^{\frac{A_9}{\lambda_3}}}{a_s \lambda_3}$	$\varepsilon_{\mathrm{BL}}^{\mathrm{F}} \approx 1 + \left(\theta e^{\theta - \frac{A_1}{\lambda_1} - \frac{A_3}{\lambda_0}} \operatorname{Ei}(-\theta) + P_{12}\right)$ $\times \left(e^{-\frac{A_8}{\lambda_3}} - \left(e^{-\frac{A_8}{\lambda_3}} - e^{-\frac{A_{10}}{\lambda_3}}\right) \left(\frac{1}{2} + \omega \vartheta\right)$ $-\frac{\omega(1 - a_s)}{a_s}\right) + \frac{\omega(1 - a_s)A_9 e^{\frac{\lambda_3}{\lambda_3}}}{a_s \lambda_3}$
$\frac{(1-a_s)\gamma_{th}}{a_s(\gamma_{th}+1)} \le \varpi$ $\le \chi \le \frac{1-a_s}{a_s}$ $\chi \le \frac{(1-a_s)\gamma_{th}}{a_s(\gamma_{th}+1)}$	$\begin{split} P_{\text{out,p}}^{\text{F}} &\approx 1 - P_{12}e^{-\frac{A_4}{\lambda_3}} - e^{-\frac{A_3}{\lambda_0} - \frac{A_4}{\lambda_3}} \left(1 - e^{-\frac{A_1}{\lambda_1}}\right) \\ &+ \left(\theta e^{\theta - \frac{A_1}{\lambda_1} - \frac{A_3}{\lambda_0}} \text{Ei} \left(-\theta\right) + P_{12}\right) \left(e^{-\frac{A_8}{\lambda_3} - \left(\frac{1}{2} + \theta \omega\right)} - \frac{\omega(1 - a_s)A_9 e^{\frac{A_9}{\lambda_3}}}{a_s \lambda_3}\right) \\ &- \frac{\omega(1 - a_s)}{a_s} \left(e^{-\frac{A_8}{\lambda_3}} - e^{-\frac{A_{10}}{\lambda_3}}\right) - \frac{\omega(1 - a_s)A_9 e^{\frac{A_9}{\lambda_3}}}{a_s \lambda_3} \\ &\times \left(\text{Ei} \left(-\frac{A_{10} + A_9}{\lambda_3}\right) - \text{Ei} \left(-\frac{A_8 + A_9}{\lambda_3}\right)\right) \\ &- P_{\text{out,p}}^{\text{F}} &\approx 1 - P_{12}e^{-\frac{A_4}{\lambda_3}} - e^{-\frac{A_3}{\lambda_0} - \frac{A_4}{\lambda_3}} \left(1 - e^{-\frac{A_1}{\lambda_1}}\right) \end{split}$	$\times \left(\operatorname{Ei} \left(-\frac{A_8 + A_9}{\lambda_3} \right) - \operatorname{Ei} \left(-\frac{A_{10} + A_9}{\lambda_3} \right) \right)$
$\frac{a_s(\gamma_{\text{th}}+1)}{\leq \frac{1-a_s}{a_s}}$ $\frac{\gamma_{\text{th}}}{1+\gamma_{\text{th}}} < a_s \leq 1$	$+\left(\theta e^{\theta-\frac{A_1}{\lambda_1}-\frac{A_3}{\lambda_0}}\operatorname{Ei}\left(-\theta\right)+P_{12}\right)e^{-\frac{A_4}{a_s\lambda_3}}$ Please refer to Table I for more details.	Please refer to Table II for more details.

For the case with $\frac{1-a_s}{a_s} \geq \chi$, there are three expressions expression of $\varepsilon_{\rm BL}^{\rm F}$. for $\Psi\left(\gamma_{{\rm IR},c}^{\rm I,F}\right)$, which are $\Psi\left(\gamma_{{\rm IR},c}^{\rm I,F}\right) \approx 1$ for $0 \leq h_3 \leq A_8$, $\Psi\left(\gamma_{{\rm IR},c}^{\rm I,F}\right) \approx \frac{1}{2} - \omega\left(\gamma_{{\rm IR},c}^{\rm I,F} - \vartheta\right)$ with $A_8 < h_3 \leq A_{10}$, and $\Psi\left(\gamma_{{\rm IR},c}^{\rm I,F}\right) \approx 0$ for $h_3 > A_{10}$, respectively. Accordingly, P_{71} Based on the abort this case is given by of this case is given by

$$P_{71} \approx 1 - e^{-\frac{A_8}{\lambda_3}} + \left(\frac{1}{2} + \omega \vartheta - \frac{\omega \left(1 - a_s\right)}{a_s}\right)$$

$$\times \left(e^{-\frac{A_8}{\lambda_3}} - e^{-\frac{A_{10}}{\lambda_3}}\right) - \frac{\omega \left(1 - a_s\right) A_9 e^{\frac{A_9}{\lambda_3}}}{a_s \lambda_3}$$

$$\times \left(\operatorname{Ei}\left(-\frac{A_8 + A_9}{\lambda_3}\right) - \operatorname{Ei}\left(-\frac{A_{10} + A_9}{\lambda_3}\right)\right). \tag{47}$$

According to the above three cases, we can obtain the

C. Summary of $P_{\text{out,p}}^{\text{F}}$ and $\varepsilon_{\text{BL}}^{\text{F}}$

Based on the above analysis, the outage probability of the primary transmission and the average BLER of AmBackCom under the improved SIC decoding scheme are summarized in Table III. As shown in Table III, we can find that the improved SIC decoding scheme can significantly improve both the outage performance of the primary transmission and the BLER performance of AmBackCom, while its outage probability and BLER can still be high, when both a_s and N_c are small, i.e., $0 \le a_s \le \frac{\gamma_{\rm th}}{1+\gamma_{\rm th}}$ and $\frac{1-a_s}{a_s} \le \varpi$. This indicates that proper a_s and N_c can be chosen to reduce both the outage probability and BLER. Although our derived expressions are too complex

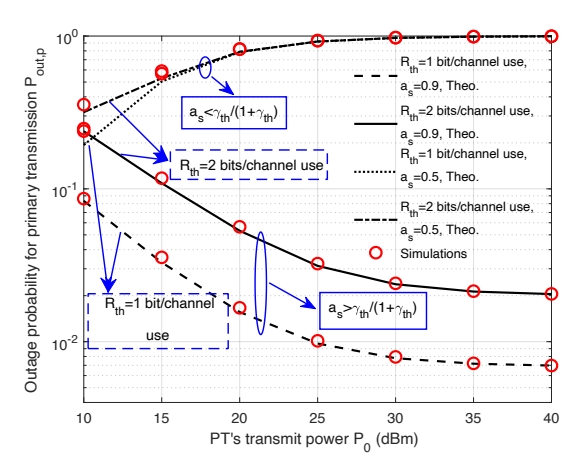


Fig. 2. Outage probability for the primary transmission versus PT's transmit power P_0 under the fixed SIC decoding scheme.

to be optimized via traditional convex optimization tools, we can use deep learning techniques, e.g., the deep reinforcement learning techniques [33], to optimize the system parameters, e.g., a_s and N_c , for performance improvement.

VI. SIMULATION AND DISCUSSION

This section is provided to evaluate the outage probability of the primary transmission and the average BLER of AmBack-Com. The basis parameters used in this paper is set following [9], [10], [22], [23]. Specifically, we set $P_0=P_{\rm R}=30$ dBm, T=1 s, $P_{\rm c}=8.9~\mu{\rm W},~N_s=50000,~N_c=400,~\sigma^2=-120$ dBm/Hz, $R_{\rm th}=2$ bits/channel use, $B_c=200$ bits, $\beta=0.8,~a_s=0.9,$ and G=10. Following a practical non-linear EH model proposed in [34], $F_{\rm NL}(P_r)$ is modeled by $F_{\rm NL}(P_r)=\frac{E_{\rm max}(1-\exp(-s_1P_r+s_1s_0))}{1+\exp(-s_1P_r+s_1s_2)},$ where $E_{\rm max}$ denotes the maximum harvestable power when the energy harvester is saturated; s_0 is the power sensitivity threshold; s_1 and s_2 are fixed parameters of the energy harvester. Based on [34], we set $E_{\rm max}=240~\mu{\rm W},~s_0=0.005,~s_1=5000,~{\rm and}~s_2=0.0002.$ Besides, we set $d_0=70$ m, $d_1=5$ m, $d_2=68$ m, $d_3=200$ m, $\alpha_0=\alpha_1=\alpha_2=\alpha_3=3,~{\rm and}~\lambda_0=\lambda_1=\lambda_2=\lambda_3=1.$

Fig. 2 shows the outage probability of the primary transmission $P_{\text{out,p}}$ versus PT's transmit power P_0 under the fixed SIC decoding scheme and different settings of $R_{\rm th}$ and a_s . Specifically, we set $R_{\rm th}$ as 2 bits/channel use and 1 bit/channel use, and a_s as 0.5 and 0.9, respectively. Note that the theoretical results for $P_{\rm out,p}$ can be obtained based on the derived expressions in Table I, while the corresponding simulation results are achieved by performing 1×10^7 Monte Carlo simulations and marked by red circles. When $a_s = 0.5$ holds, we have $a_s \leq \frac{\gamma_{\rm th}}{1+\gamma_{\rm th}}$ and the values of $P_{\rm out,p}$ are computed based on the expression of $P_{\rm out,p}$ under the case with $0 \le a_s \le \frac{\gamma_{\rm th}}{1+\gamma_{\rm th}}$ in Table I. Similarly, when $a_s = 0.9$ holds, we have $a_s > \frac{\gamma_{\rm th}}{1+\gamma_{\rm th}}$ and we calculate the values of $P_{\text{out,p}}$ based on the expression of $P_{\text{out,p}}$ under the case with $\frac{\gamma_{\rm th}}{1+\gamma_{\rm th}} < a_s \leq 1$ in Table I. It can be observed that our derived theoretical results match well with the simulation results, which demonstrates the accuracy of the outage probabilities we have derived in Table I. Besides, we can also see that with the increasing P_0 , $P_{\rm out,p}$ under the case with $a_s \leq \frac{\gamma_{\rm th}}{1+\gamma_{\rm th}}$

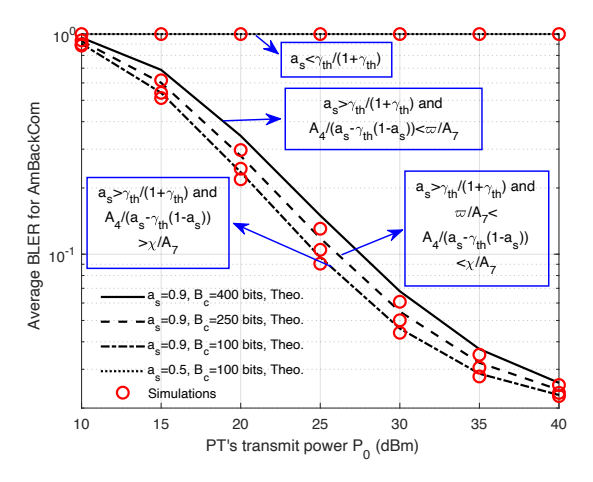


Fig. 3. Average BLER for AmBackCom versus P_0 under the fixed SIC decoding scheme.

increases first and then converges to 1 while $P_{\mathrm{out,p}}$ under the case with $a_s > \frac{\gamma_{\mathrm{th}}}{1+\gamma_{\mathrm{th}}}$ decreases first and then converges to a certain value. The reasons are as follows. With $a_s \leq \frac{\gamma_{\mathrm{th}}}{1+\gamma_{\mathrm{th}}}$, when P_0 increases, R has a larger probability to decode s and c successfully, leading to a smaller P_2 and P_3 . Since in this case, IR always fails to decode \hat{s} , P_1 also becomes smaller. Thus, there is an upward trend in $P_{\mathrm{out,p}}$. When P_0 is large enough, P_1 , P_2 and P_3 become 0, leading to $P_{\mathrm{out,p}} = 1$. With $a_s > \frac{\gamma_{\mathrm{th}}}{1+\gamma_{\mathrm{th}}}$, when P_0 increases, P_1 who is the dominant factor to $P_{\mathrm{out,p}}$ becomes larger, leading to a smaller $P_{\mathrm{out,p}}$. This is because $P_{\mathrm{out,p}}$ decreases with the increase of $P_{\mathrm{suc,p}}$ and (13) shows a larger P_1 resulting in a larger $P_{\mathrm{suc,p}}$. Therefore, $P_{\mathrm{out,p}}$ decreases with the increasing P_0 . With a larger P_0 , there exists an error floor caused by the interference from BT.

Fig. 3 plots the average BLER for AmBackCom $\varepsilon_{\rm BL}$ versus P_0 under the fixed SIC decoding scheme, where a_s is set as 0.5 and 0.9, and B_c is set as 100 bits, 250 bits and 400 bits. Note that the theoretical results for $\varepsilon_{\rm BL}$ are computed based on the derived expressions in Table II. According to Table II, there are four expressions to calculate $\varepsilon_{\mathrm{BL}}$ for different settings of a_s and B_c . Specifically, with $a_s = 0.9$ and $B_c = 400$ bits, we have $a_s>\frac{\gamma_{\rm th}}{1+\gamma_{\rm th}}$ and $\frac{A_4}{a_s-\gamma_{\rm th}(1-a_s)}<\frac{\varpi}{A_7}.$ With $a_s=0.9$ and $B_c=250$ bits, both $a_s>\frac{\gamma_{\rm th}}{1+\gamma_{\rm th}}$ and $\frac{\varpi}{A_7}<\frac{A_4}{a_s-\gamma_{\rm th}(1-a_s)}<\frac{\chi}{A_7}$ hold. With $a_s=0.9$ and $B_c=100$ bits, we can obtain $a_s>0$ $\frac{\gamma_{\rm th}}{1+\gamma_{\rm th}}$ and $\frac{A_4}{a_s-\gamma_{\rm th}(1-a_s)}>\frac{\lambda}{A_7}$. With $a_s=0.5$ and $B_c=100$ bits, we have $a_s<\frac{\gamma_{\rm th}}{\gamma_{\rm th}}$. The corresponding closed-form can be found in Table II. Through a comparison with simulation results, we have confirmed the accuracy of the average BLER values derived in Table II. Besides, we can see that with the increasing P_0 , $\varepsilon_{\rm BL}$ under the case with $a_s < \frac{\gamma_{\rm th}}{1+\gamma_{\rm th}}$ is always 1 while $\varepsilon_{\rm BL}$ under the case with $a_s > \frac{\gamma_{\rm th}}{1+\gamma_{\rm th}}$ will decrease. This is because when $a_s < \frac{\gamma_{\rm th}}{1+\gamma_{\rm th}}$ holds, IR fails to either receive \widehat{c} or decode \widehat{s} , so that \widehat{c} can also not be decoded at IR. Leading to the second of the contraction of the second of IR, leading to $\varepsilon_{\rm BL}=1.$ As for the case with $a_s>\frac{\gamma_{\rm th}}{1+\gamma_{\rm th}},$ when P_0 increases, BT has a larger probability to backscatter information and both R and IR have larger probabilities to decode the backscattered information successfully, leading to a reduction of $\varepsilon_{\rm BL}$.

Fig. 4 shows the outage probability for the primary trans-

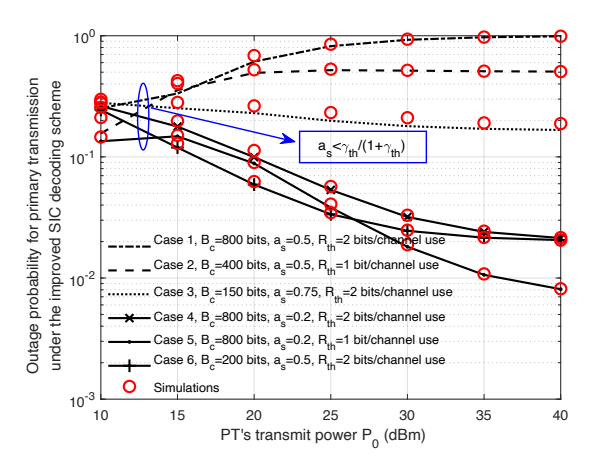


Fig. 4. Outage probability for the primary transmission under the improved SIC decoding scheme versus P_0 .

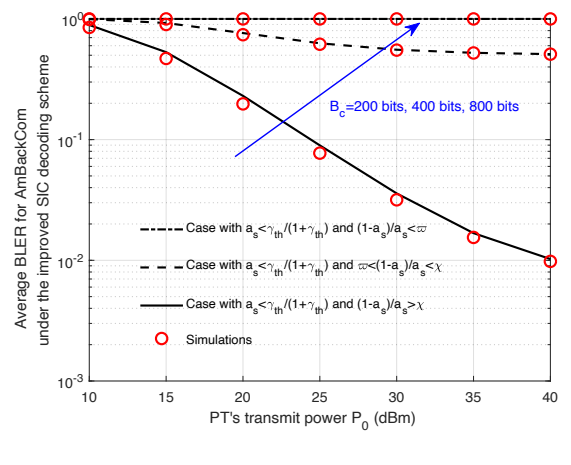


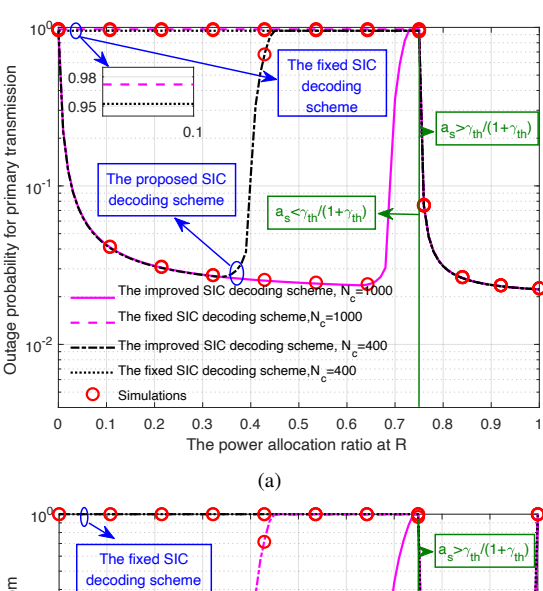
Fig. 5. Average BLER for AmBackCom under the improved SIC decoding scheme versus P_0 .

mission with the improved SIC decoding scheme $P_{\text{out,p}}^{\text{F}}$ versus P_0 under different settings of B_c , a_s and $R_{\rm th}$. Specifically, when $B_c=800$ bits, $a_s=0.5$ and $R_{\rm th}=2$ bits/channel use are satisfied, both $a_s<\frac{\gamma_{\rm th}}{1+\gamma_{\rm th}}$ and $\frac{1-a_s}{a_s}\leq \varpi$ hold, namely the condition of Case 1 in Section V.A is satisfied. With $B_c=400$ bits, $a_s=0.5$ and $R_{\rm th}=1$ bit/channel use, we have $a_s=\frac{\gamma_{\rm th}}{1+\gamma_{\rm th}}$ and $\frac{(1-a_s)\gamma_{\rm th}}{a_s(\gamma_{\rm th}+1)}\leq\varpi\leq\frac{1-a_s}{a_s}\leq\chi$, which meets the condition of Case 2 in Section V.A. As for $B_c=150$ bits, $a_s=0.75$ and $R_{\rm th}=2$ bits/channel use, we can obtain $a_s=\frac{\gamma_{\rm th}}{1+\gamma_{\rm th}}$ and $\varpi\leq\frac{(1-a_s)\gamma_{\rm th}}{a_s(\gamma_{\rm th}+1)}\leq\frac{1-a_s}{a_s}\leq\chi$, satisfying the condition of Case 3 in Section V.A. When $B_c=800$ bits, $a_s=0.2$ and $R_{\rm th}=2$ bits/channel use hold, we obtain $a_s<\frac{\gamma_{\rm th}}{1+\gamma_{\rm th}}$ and $\varpi\leq\frac{(1-a_s)\gamma_{\rm th}}{a_s(\gamma_{\rm th}+1)}\leq\chi\leq\frac{1-a_s}{a_s}$, bringing the condition of Case 4 in Section V.A. In order to achieve $a_s<\frac{\gamma_{\rm th}}{1+\gamma_{\rm th}}$ and $\frac{(1-a_s)\gamma_{\rm th}}{a_s(\gamma_{\rm th}+1)}\leq\varpi\leq\chi\leq\frac{1-a_s}{a_s}$ (i.e., the condition of Case 5 in Section V.A), we set $B_c=800$ bits, $a_s = 0.2$ and $R_{\rm th} = 1$ bit/channel use. Similarly, to meet the condition of Case 6 in Section V.A ($a_s < \frac{\gamma_{\rm th}}{1+\gamma_{\rm th}}$ and $\chi \leq \frac{(1-a_s)\gamma_{\rm th}}{a_s(\gamma_{\rm th}+1)} \leq \frac{1-a_s}{a_s}$), we set $B_c=200$ bits, $a_s=0.5$ and $R_{
m th}=2$ bits/channel use. Then the theoretical results of $P_{
m out,p}^{
m F}$ can be calculated based on the expressions under the above cases in Table III. By comparing the theoretical results with the simulation results, the correctness of our derived expressions for $P_{\text{out,p}}^{\text{F}}$ in Table III is illustrated. Besides, it can also be observed that $P_{\text{out,p}}^{\text{F}}$ in Case 1 and Case 2 increases with P_0 and then converges to 1, while $P_{\text{out,p}}^{\text{F}}$ in the others shows a downward trend. The reasons are as follows. In Case 1 and Case 2, IR has a smaller probability to decode \hat{c} successfully, leading to a smaller P_6 . Among P_6 , P_2 and P_3 , P_3 becomes the dominant factor to $P_{\text{out,p}}^{\text{F}}$ and decreases with P_0 , leading to an increasing $P_{\text{out,p}}^{\text{F}}$. When P_0 becomes large enough, P_6 , P_2 and P_3 go to zero, bringing $P_{\text{out,p}}^{\text{F}} = 1$. In Case 3, Case 4, Case 5 and Case 6, P_6 is the dominant factor to $P_{\text{out,p}}^{\text{F}}$ and increases with P_0 , so that $P_{\text{out,p}}^{\text{F}}$ decreases when P_0 increases.

Fig. 5 shows the average BLER for AmBackCom under the improved SIC decoding scheme $\varepsilon_{\rm BL}^{\rm F}$ versus P_0 , where $a_s=0.5,\ R_{\rm th}=1$ bit/channel use, and B_c is set as 200 bits, 400 bits and 800 bits, respectively. In particular, with $B_c=200$ bits, we have $a_s<\frac{\gamma_{\rm th}}{1+\gamma_{\rm th}}$ and $\frac{1-a_s}{a_s}<\varpi$. With

 $B_c=400$ bits, both $a_s<\frac{\gamma_{\mathrm{th}}}{1+\gamma_{\mathrm{th}}}$ and $\varpi<\frac{1-a_s}{a_s}<\chi$ hold. With $B_c=800$ bits, both $a_s<\frac{\gamma_{\mathrm{th}}}{1+\gamma_{\mathrm{th}}}$ and $\frac{1-a_s}{a_s}>\chi$ are satisfied. Then the theoretical results of $\varepsilon_{\mathrm{BL}}^{\mathrm{F}}$ are calculated according to the corresponding expressions under the above cases in Table III. As shown in this figure, we can see that the theoretical results match well with the simulation results, showing the correctness of our derived expressions for $\varepsilon_{\mathrm{BL}}^{\mathrm{F}}$ in Table III. Another observation is that with the increasing B_c , $\varepsilon_{\mathrm{BL}}^{\mathrm{F}}$ also increases and when B_c is large enough, $\varepsilon_{\mathrm{BL}}^{\mathrm{F}}=1$ always holds. Combining with Fig. 3, we can find that the improved SIC decoding scheme can reduce the average BLER of AmBackCom efficiently, illustrating the advantage of the improved SIC decoding scheme.

Fig. 6 shows the impact of the power allocation ratio at R a_s on the outage probability for the primary transmission and the average BLER for AmBackCom, where both the fixed SIC decoding scheme and the improved SIC decoding scheme are considered at IR. We set B_c as 500 bits and N_c as 400 and 1000. Fig. 6(a) plots the outage probability for the primary transmission versus a_s under the fixed SIC decoding scheme and the improved SIC decoding scheme. It can be observed that $P_{\mathrm{out,p}}^{\mathrm{F}}$ decreases first, reaches its minimum and then increases when $a_s < \frac{\gamma_{\mathrm{th}}}{1+\gamma_{\mathrm{th}}}$ holds. With $a_s > \frac{\gamma_{\mathrm{th}}}{1+\gamma_{\mathrm{th}}}$, $P_{
m out,p}^{
m F}$ decreases first and then converges to its minimum value. This is due to the fact that with $a_s < \frac{\gamma_{\rm th}}{1+\gamma_{\rm th}}$, when a_s increases, $\gamma_{{
m IR},s}^{{
m I,F}}$ also increases, bringing a larger probability that \widehat{s} is successfully decoded. When a_s is large enough, $\gamma_{{\rm IR},c}^{{
m I,F}}$ becomes small. This brings a small probability to decode \widehat{c} successfully, so that the probability that \widehat{s} is successfully decoded is also small. With $a_s > \frac{\gamma_{\rm th}}{1+\gamma_{\rm th}}$, $\gamma_{\rm IR,s}^{\rm I}$ will increase when a_s increases, bringing a reduction of $P_{\rm out,p}^{\rm F}$, and when a_s achieves its maximum value, $P_{\mathrm{out,p}}^{\mathrm{F}}$ also achieves its minimum value. As for the fixed SIC decoding scheme, $P_{\text{out,p}}$ keeps unchanged for $a_s < \frac{\gamma_{\rm th}}{1+\gamma_{\rm th}}$. This is because with $a_s < \frac{\gamma_{\rm th}}{1+\gamma_{\rm th}}$, $P_{\rm out,p}$ is decided by $1-P_2-P_3$, which is irrelevant to a_s . With $a_s > \frac{\gamma_{\rm th}}{1+\gamma_{\rm th}}$, it has the same behavior with $P_{\rm out,p}^{\rm F}$. By comparisons, we can observe that the improved SIC decoding scheme can significantly improve the outage performance for the primary transmission under the case with $a_s \leq \frac{\gamma_{\rm th}}{1+\gamma_{\rm th}}$,



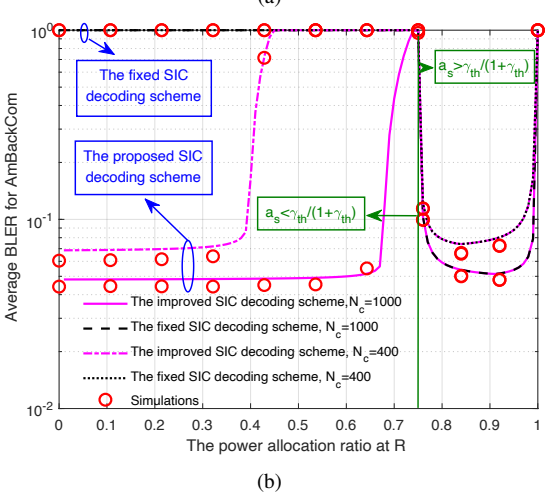


Fig. 6. The impact of the power allocation ratio at R on the outage probability for the primary transmission and the average BLER for AmBackCom.

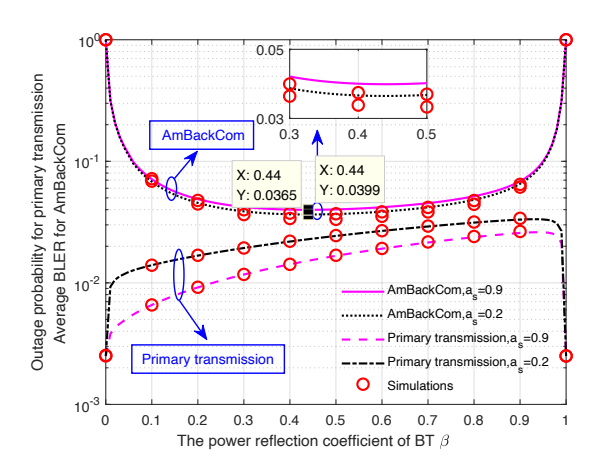


Fig. 7. Outage probability for the primary transmission/average BLER for AmBackCom versus the power reflection coefficient of BT β under the improved SIC decoding scheme.

demonstrating the superiority of the improved SIC decoding scheme in terms of the outage probability for the primary transmission.

Fig. 6(b) shows the average BLER for AmBackCom versus a_s under the fixed SIC decoding scheme and the improved SIC decoding scheme. It can be seen that with $a_s < \frac{\gamma_{\rm th}}{1+\gamma_{\rm th}}$, $\varepsilon_{\rm BL}^{\rm F}$

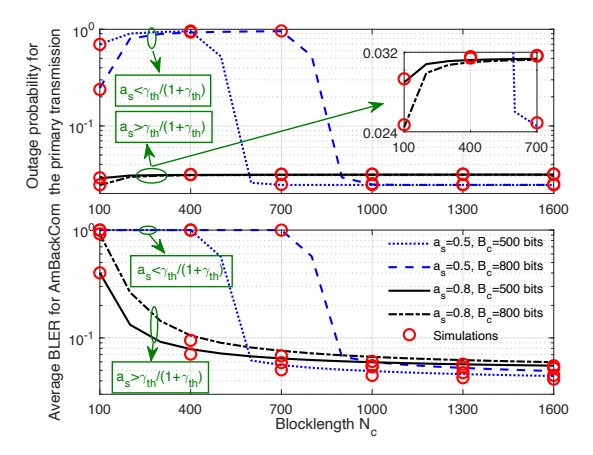


Fig. 8. Outage probability for the primary transmission/average BLER for AmBackCom versus the short-packect blocklength N_c under the improved SIC decoding scheme.

increases with a_s and when $a_s > \frac{\gamma_{\rm th}}{1+\gamma_{\rm th}}$ holds, $\varepsilon_{\rm BL}^{\rm F}$ decreases first, reaches its minimum, and then increases until $\varepsilon_{\rm BL}^{\rm F}=1$. The reasons are as follows. With $a_s < \frac{\gamma_{\rm th}}{1+\gamma_{\rm th}}$, a larger a_s means a smaller $\gamma_{\rm IR,c}^{\rm I,F}$, leading to an improvement of $\varepsilon_{\rm BL}^{\rm F}$. When $a_s > \frac{\gamma_{\rm th}}{1+\gamma_{\rm th}}$, with a smaller a_s , $\gamma_{\rm IR,s}^{\rm I}$ is smaller, bringing smaller probabilities for decoding \widehat{s} and \widehat{c} successfully. When a_s is large enough, $\gamma_{\rm IR,c}^{\rm I}$ becomes very small, leading to an improvement to $\varepsilon_{\rm BL}^{\rm F}$. As for the fixed SIC decoding scheme, $\varepsilon_{\rm BL}=1$ always holds for $a_s < \frac{\gamma_{\rm th}}{1+\gamma_{\rm th}}$. This is because with $a_s < \frac{\gamma_{\rm th}}{1+\gamma_{\rm th}}$, \widehat{c} is always decoded unsuccessfully due to the failed decoding of \widehat{s} , leading to $\varepsilon_{\rm BL}=1$. For $a_s > \frac{\gamma_{\rm th}}{1+\gamma_{\rm th}}$, $\varepsilon_{\rm BL}$ has the same behavior with $\varepsilon_{\rm BL}^{\rm F}$. By comparisons, we can also see that $\varepsilon_{\rm BL}^{\rm F}$ is always lower than $\varepsilon_{\rm BL}$ when $a_s < \frac{\gamma_{\rm th}}{1+\gamma_{\rm th}}$, which verifies the advantage of the improved SIC decoding scheme in terms of the average BLER for AmBackCom. Combining Fig. 6(a) and Fig. 6(b), it can be found that the improved SIC decoding scheme brings performance improvements for both PT's and BT's information transmissions.

Fig. 7 shows the outage probability for the primary transmission/average BLER for AmBackCom versus the power reflection coefficient of BT β under the improved SIC decoding scheme, where a_s is set as 0.9 and 0.2, respectively. As shown in this figure, we can see that when β increases, $P_{\text{out,p}}^F$ increases first, reaches its peak and then decreases, while $\varepsilon_{\text{BL}}^F$ decreases first, achieves its minimum value and then increases. The reasons are as follows. With a larger β , the signal backscattered by BT becomes stronger, leading to a higher $P_{\text{out,p}}^F$ and a lower $\varepsilon_{\text{BL}}^F$. When β is large enough, BT has a small probability to perform AmBackCom, bringing a lower $P_{\text{out,p}}^F$ and a higher $\varepsilon_{\text{BL}}^F$. Another observation is that $P_{\text{out,p}}^F$ can achieve its minimum value when $\beta=0$ or 1 holds since PT's transmission is not interfered by AmBackCom. Besides, there exists an optimal β that minimizes $\varepsilon_{\text{BL}}^F$.

Fig. 8 shows the outage probability for the primary transmission and the average BLER for AmBackCom versus the short-packet blocklength N_c under the improved SIC decoding scheme, where a_s is set as 0.5 and 0.8, and B_c is set as 500 bits and 800 bits. From the upper figure in Fig. 8, we can observe that with the increasing N_c , $P_{\text{out,p}}^{\text{F}}$ first increases and then

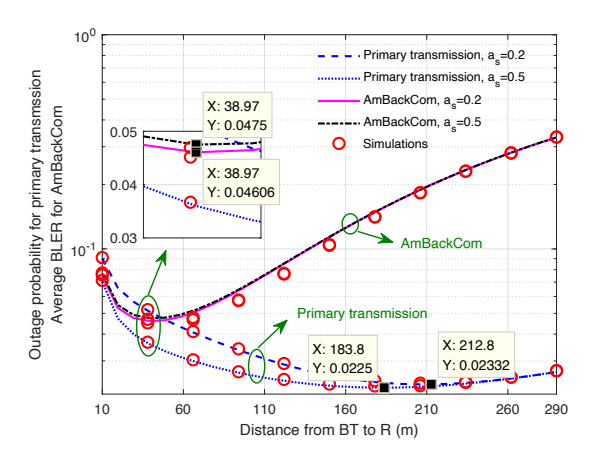


Fig. 9. Outage probability for the primary transmission/average BLER for AmBackCom versus the distance from BT to R d_2 under the improved SIC decoding scheme.

decreases until it reaches a certain value for the case with $a_s < \frac{\gamma_{\rm th}}{1+\gamma_{\rm th}}$, while it first increases and then converges to a certain value for the case with $a_s > \frac{\gamma_{\rm th}}{1+\gamma_{\rm th}}$. The reason is as follows. In the case with $a_s < \frac{\gamma_{\rm th}}{1+\gamma_{\rm th}}$, a larger N_c results in smaller $\varepsilon_{\rm R,c}$ and $\varepsilon_{\rm IR,c}^{\rm F}$, leading to a smaller P_2 and a larger P_6 . Since P_2 is the dominant factor $P_{\rm out,p}^{\rm F}$ when N_c is small and the impact of P_6 increases as N_c increases, $P_{\rm out,p}^{\rm F}$ first increases and then decreases. When N_c is large enough, P_2 approaches to 0 and P_6 approaches to $\mathbb{P}\left(E_{\rm BT} \geq \frac{P_c T}{2}, \gamma_{\rm R,s}^a \geq \gamma_{\rm th}, \gamma_{\rm IR,s}^{\rm I,F} \geq \gamma_{\rm th}\right)$, which is not related with N_c . In the case with $a_s > \frac{\gamma_{\rm th}}{1+\gamma_{\rm th}}$, as N_c increases, P_1 increases and P_2 decreases. Since the impact of P_1 is lower than that of P_2 , there is an upward trend for $P_{\rm out,p}^{\rm F}$. Similarly, with a larger N_c , $P_{\rm out,p}^{\rm F}$ becomes irrelevant to N_c . Based on the above observations, we can find that a smaller N_c may bring a reduction of N_c on N_c . Besides, we can also see that the impact of N_c on N_c is also affected by the value of N_c and different settings of N_c brings different impacts. From the lower figure, we can see that $\varepsilon_{\rm BL}^{\rm F}$ always decreases with the increasing N_c until it converges to a certain value. This is because a larger N_c brings smaller $\varepsilon_{\rm R,c}$ and $\varepsilon_{\rm IR,c}$, resulting in a smaller $\varepsilon_{\rm BL}^{\rm F}$. When N_c is large enough, $\varepsilon_{\rm BL}^{\rm F}$ becomes irrelevant to N_c . On this basis, we can find that a larger N_c is required to achieve a smaller $\varepsilon_{\rm BL}^{\rm F}$.

Fig. 9 shows the outage probability for the primary transmission and the average BLER for AmBackCom versus the distance from BT to R d_2 under the improved SIC decoding scheme, where a_s is set as 0.2 and 0.5, and $R_{\rm th}$ is set as 1 bit/channel use. Here d_1 is set as 5 m, and d_2 varies from 10 m to 290 m. d_0 and d_3 are given by $d_1 + d_2$ and $300 - d_2$, respectively. It can be observed that both $P_{\mathrm{out,p}}^{\mathrm{F}}$ and $arepsilon_{\mathrm{BL}}^{\mathrm{F}}$ first decrease, reach the minimum and then increase when d_2 increases. This indicates that there exist two optimal values of d_2 that make $P_{\mathrm{out,p}}^{\mathrm{F}}$ or $\varepsilon_{\mathrm{BL}}^{\mathrm{F}}$ minimum, respectively. The reasons are as follows. For both the primary transmission and AmBackCom, a larger d_2 means a larger d_0 and a smaller d_3 , which results in smaller probabilities that R can decode s and c, as well as larger probabilities that IR can decode \hat{s} and \hat{c} . According to the principle of the DF protocol, the minimum $P_{\mathrm{out,p}}^{\mathrm{F}}$ or $\varepsilon_{\mathrm{BL}}^{\mathrm{F}}$ can be achieved when the successful transmission probability of the PT/BT-to-R link is equal to that of the R-to-IR link. Another observation is that the optimal value of d_2 that minimizes $\varepsilon_{\rm BL}^{\rm F}$ is smaller than that minimizes $P_{\rm out,p}^{\rm F}$. For example, with the same parameter settings, i.e., $a_s=0.2,\,\varepsilon_{\rm BL}^{\rm F}$ is minimized when d_2 is about 38.97 m while d_2 should be around 212.8 m for minimizing $P_{\rm out,p}^{\rm F}$. This is due to the fact that the backscattered signal c from BT suffers from a phenomenon known as "double fading", leading to a poor $\varepsilon_{\rm BL}^{\rm F}$. Since the deployment of R close to BT can enhance its received power of the backscattered signal, a small d_2 is preferred to minimize $\varepsilon_{\rm BL}^{\rm F}$.

VII. CONCLUSION

In this work, we have proposed and studied a relay assisted cooperative AmBackCom network, where a relay node is deployed to forward the long packets emitted by PT and the short packets conveyed by BT. In particular, the expressions for PT's outage probability and BT's BLER have been derived by considering the energy causal constraint and the decoding error of a fixed SIC decoding scheme. It has been found that the fixed SIC decoding scheme leads to a high outage probability and BLER if the power allocation ratio is not well-selected. To solve it, we have further proposed an improved SIC decoding scheme, where IR can first decode BT's information when it fails to decode PT's information. The closed-form expressions for PT's outage probability and BT's BLER have been derived to assess the performance of the improved SIC decoding scheme. Simulation results have been provided to verify the correctness of the derived expressions, to show the advantages of the improved SIC decoding scheme, and to find insights that have been summarized in Section I.

There are three future directions to be explored. First, based on the derived expressions, the optimization schemes can be designed by means of deep reinforcement learning techniques to further reduce the outage probability of the primary transmission or the average BLER of AmBackCom. Second, it will be interesting to introduce an automatic repeat request (ARQ) technique, e.g., incremental redundancy hybrid ARQ (IR-HARQ), into the short-packet AmBackCom and reanalyze the BLER. Third, the outage performance of the primary transmission and the average BLER of AmBackCom will be reanalyzed when considering reconfigurable intelligent surfaces instead of a DF relay.

REFERENCES

- L. Chettri and R. Bera, "A comprehensive survey on internet of things IoT toward 5G wireless systems," *IEEE Internet Things J.*, vol. 7, no. 1, pp. 16–32, 2020.
- [2] Y. Ye, L. Shi, X. Chu, R. Q. Hu, and G. Lu, "Resource allocation in backscatter-assisted wireless powered MEC networks with limited MEC computation capacity," *IEEE Trans. Wireless Commun.*, vol. 21, no. 12, pp. 10678–10694, 2022.
- [3] B. Gu, D. Li, and H. Xie, "Computation-efficient backscatter-blessed MEC with user reciprocity," *IEEE Trans. Veh. Technol.*, pp. 1–6, 2023.
- [4] N. V. Huynh, D. T. Hoang, X. Lu, D. Niyato, P. Wang, and D. I. Kim, "Ambient backscatter communications: A contemporary survey," *IEEE Commun. Surv. Tutor.*, vol. 20, no. 4, pp. 2889–2922, 2018.
- [5] Y. Ye, L. Shi, R. Qingyang Hu, and G. Lu, "Energy-efficient resource allocation for wirelessly powered backscatter communications," *IEEE Commun. Lett.*, vol. 23, no. 8, pp. 1418–1422, Aug 2019.

- [6] L. Xu, K. Zhu, R. Wang, and S. Gong, "Performance analysis of ambient backscatter communications in RF-powered cognitive radio networks," in *Proc. IEEE WCNC*, April 2018, pp. 1–6.
- [7] S. T. Shah, K. W. Choi, T. Lee, and M. Y. Chung, "Outage probability and throughput analysis of SWIPT enabled cognitive relay network with ambient backscatter," *IEEE Internet Things J.*, vol. 5, no. 4, pp. 3198– 3208, Aug 2018.
- [8] X. Lu, H. Jiang, D. Niyato, D. I. Kim, and Z. Han, "Wireless-powered device-to-device communications with ambient backscattering: Performance modeling and analysis," *IEEE Trans. Wireless Commun.*, vol. 17, no. 3, pp. 1528–1544, March 2018.
- [9] Y. Ye, L. Shi, X. Chu, and G. Lu, "On the outage performance of ambient backscatter communications," *IEEE Internet Things J.*, vol. 7, no. 8, pp. 7265–7278, 2020.
- [10] L. Shi, R. Q. Hu, Y. Ye, and H. Zhang, "Modeling and performance analysis for ambient backscattering underlaying cellular networks," *IEEE Trans. Veh. Technol.*, vol. 69, no. 6, pp. 6563–6577, 2020.
- [11] H. Ding, D. B. da Costa, and J. Ge, "Outage analysis for cooperative ambient backscatter systems," *IEEE Wireless Commun. Lett.*, vol. 9, no. 5, pp. 601–605, 2020.
- [12] Y. Liu, Y. Ye, G. Yan, and Y. Zhao, "Outage performance analysis for an opportunistic source selection based two-way cooperative ambient backscatter communication system," *IEEE Commun. Lett.*, vol. 25, no. 2, pp. 437–441, 2021.
- [13] S. Zhou, W. Xu, K. Wang, C. Pan, M.-S. Alouini, and A. Nallanathan, "Ergodic rate analysis of cooperative ambient backscatter communication," *IEEE Wireless Commun. Lett.*, vol. 8, no. 6, pp. 1679–1682, 2019.
- [14] H. Ding, M.-S. Alouini, K. Xin, H. Li, and S. Xu, "Symbiotic ambient backscatter systems: Outage behavior and ergodic capacity," *IEEE Internet Things J.*, vol. 9, no. 23, pp. 23 670–23 690, 2022.
- [15] W. Zhao, J. Zhu, X. She, G. Wang, and C. Tellambura, "Ergodic capacity analysis for cooperative ambient communication system under sensitivity constraint," *IEEE Commun. Lett.*, pp. 1–1, 2023.
- [16] Z. Yang, L. Feng, F. Zhou, X. Qiu, and W. Li, "Analytical performance analysis of intelligent reflecting surface aided ambient backscatter communication network," *IEEE Wireless Commun. Lett.*, vol. 10, no. 12, pp. 2732–2736, 2021.
- [17] Y. Chen, "Performance of ambient backscatter systems using reconfigurable intelligent surface," *IEEE Commun. Lett.*, vol. 25, no. 8, pp. 2536– 2539, 2021.
- [18] M. Elsayed, A. Samir, A. A. A. El-Banna, X. Li, and B. M. ElHalawany, "When NOMA multiplexing meets symbiotic ambient backscatter communication: Outage analysis," *IEEE Trans. Veh. Technol.*, vol. 71, no. 1, pp. 1026–1031, 2022.
- [19] G. Durisi, T. Koch, J. stman, Y. Polyanskiy, and W. Yang, "Short-packet communications over multiple-antenna rayleigh-fading channels," *IEEE Trans. Commun.*, vol. 64, no. 2, pp. 618–629, 2016.
- [20] Y. Polyanskiy, H. V. Poor, and S. Verdu, "Channel coding rate in the finite blocklength regime," *IEEE Trans. Inf. Theory*, vol. 56, no. 5, pp. 2307–2359, 2010.
- [21] G. Durisi, T. Koch, and P. Popovski, "Toward massive, ultrareliable, and low-latency wireless communication with short packets," *Proc. IEEE*, vol. 104, no. 9, pp. 1711–1726, 2016.
- [22] X. Lu, P. Wang, G. Li, D. Niyato, and Z. Li, "Short-packet backscatter assisted wireless-powered relaying with NOMA: Mode selection with performance estimation," *IEEE Trans. Cognit. Commun. Netw.*, vol. 8, no. 1, pp. 216–231, 2022.
- [23] L. Zhang and Y.-C. Liang, "Average throughput analysis and optimization in cooperative iot networks with short packet communication," *IEEE Trans. Veh. Technol.*, vol. 67, no. 12, pp. 11549–11562, 2018.
- [24] Z. Chu, W. Hao, P. Xiao, M. Khalily, and R. Tafazolli, "Resource allocations for symbiotic radio with finite blocklength backscatter link," *IEEE Internet Things J.*, vol. 7, no. 9, pp. 8192–8207, 2020.
- [25] Z. Zhao, Y. Cai, W. Hong, J. Jiang, M. Peng, and T. Q. S. Quek, "On the design of backscatter communications with retransmissions," *IEEE Wireless Commun. Lett.*, vol. 11, no. 12, pp. 2555–2559, 2022.
- [26] R. Xu, L. Shi, Y. Ye, H. Sun, and G. Zheng, "Relay-enabled backscatter communications: Linear mapping and resource allocation," *IEEE Trans. Veh. Technol.*, pp. 1–15, 2023.
- [27] X. Li, J. Jiang, H. Wang, C. Han, G. Chen, J. Du, C. Hu, and S. Mumtaz, "Physical layer security for wireless-powered ambient backscatter cooperative communication networks," *IEEE Trans. Cognit. Commun. Netw.*, vol. 9, no. 4, pp. 927–939, 2023.
- [28] S. Gong, L. Gao, J. Xu, Y. Guo, D. T. Hoang, and D. Niyato, "Exploiting backscatter-aided relay communications with hybrid access model in device-to-device networks," *IEEE Trans. Cognit. Commun. Netw.*, vol. 5, no. 4, pp. 835–848, 2019.

- [29] S. Gong, Y. Zou, D. T. Hoang, J. Xu, W. Cheng, and D. Niyato, "Capitalizing backscatter-aided hybrid relay communications with wireless energy harvesting," *IEEE Internet Things J.*, vol. 7, no. 9, pp. 8709–8721, 2020.
- [30] Z. B. Zawawi, Y. Huang, and B. Clerckx, "Multiuser wirelessly powered backscatter communications: Nonlinearity, waveform design, and SINRenergy tradeoff," *IEEE Trans. Wireless Commun.*, vol. 18, no. 1, pp. 241–253, 2019.
- [31] I. S. Gradshteyn and I. M. Ryzhik, Table of integrals, series, and products, Academic press, 2014.
- [32] X. Lai, T. Wu, Q. Zhang, and J. Qin, "Average secure BLER analysis of NOMA downlink short-packet communication systems in flat rayleigh fading channels," *IEEE Trans. Wireless Commun.*, vol. 20, no. 5, pp. 2948–2960, 2021.
- [33] W. Xu, Z. Yang, D. W. K. Ng, M. Levorato, Y. C. Eldar, and M. Debbah, "Edge learning for B5G networks with distributed signal processing: Semantic communication, edge computing, and wireless sensing," *IEEE J. Sel. Topics Signal Process.*, vol. 17, no. 1, pp. 9–39, 2023.
- [34] S. Wang, M. Xia, K. Huang, and Y. Wu, "Wirelessly powered two-way communication with nonlinear energy harvesting model: Rate regions under fixed and mobile relay," *IEEE Trans. Wireless Commun.*, vol. 16, no. 12, pp. 8190–8204, Dec 2017.